Trajectory of plasma lipidome associated with the risk of late-onset Alzheimer's disease: a longitudinal cohort study

Tingting Wang,[a,b,o] Matthias Arnold,[c,d,o] Kevin Huynh,[a,b,e,o] Patrick Weinisch,[d] Corey Giles,[a,b,e] Natalie A. Mellett,[a] Thy Duong,[a] Bharadwaj Marella,[d] Kwangsik Nho,[f,g,h] Alysha De Livera,[i] Xianlin Han,[j] Colette Blach,[k] Chenglong Yu,[l] John J. McNeil,[l] Paul Lacaze,[l] Andrew J. Saykin,[f,h] Gabi Kastenmüller,[d,p] Peter J. Meikle,[a,b,e,p] and Rima Kaddurah-Daouk,[c,m,n,p,*] for the Alzheimer's Disease Neuroimaging Initiative (ADNI)[q]

[a]Baker Heart and Diabetes Institute, Melbourne, Australia
[b]Baker Department of Cardiometabolic Health, University of Melbourne, Victoria, Australia
[c]Department of Psychiatry and Behavioral Sciences, Duke University, Durham, NC, USA
[d]Institute of Computational Biology, Helmholtz Zentrum München, German Research Center for Environmental Health, Neuherberg, Germany
[e]Department of Cardiovascular Research Translation and Implementation, La Trobe University, Melbourne, Australia
[f]Department of Radiology and Imaging Sciences, Indiana University School of Medicine, Indianapolis, IN, USA
[g]Center for Computational Biology and Bioinformatics, Indiana University School of Medicine, Indianapolis, IN, USA
[h]Indiana Alzheimer Disease Center, Indiana University School of Medicine, Indianapolis, IN, USA
[i]School of Computing, Engineering and Mathematical Sciences, La Trobe University, Melbourne, Australia
[j]Barshop Institute for Longevity and Aging Studies, University of Texas Health Science Center at San Antonio, San Antonio, TX, USA
[k]Duke Molecular Physiology Institute, Duke University, Durham, NC, USA
[l]School of Public Health and Preventive Medicine, Monash University, Melbourne, VIC, Australia
[m]Duke Institute of Brain Sciences, Duke University, Durham, NC, USA
[n]Department of Medicine, Duke University, Durham, NC, USA

eBioMedicine
2025;118: 105826
Published Online xxx
https://doi.org/10.1016/j.ebiom.2025.105826

Summary

Background Comprehensive lipidomic studies have demonstrated strong cross-sectional associations between the blood lipidome and late-onset Alzheimer's disease (AD) dementia and its risk factors, yet the longitudinal relationship between lipidome changes and AD progression remains unclear.

Methods We employed longitudinal lipidomic profiling on 4730 plasma samples from 1517 participants of the Alzheimer's Disease Neuroimaging Initiative (ADNI) cohort to investigate the temporal evolution of lipidomes among diagnostic groups. At baseline (n = 1393), participants were classified as stable diagnosis status including stable AD (n = 243), stable cognitive normal (CN; n = 337), and stable mild cognitive impairment (MCI; n = 413), or converters (AD converters: n = 329; MCI converters: n = 71). We developed a dementia risk classification model to stratify the non-converting MCI group into dementia-like and non-dementia-like MCI based on their baseline lipidomic profiles, aiming to identify early metabolic signatures predictive of dementia progression.

Findings Longitudinal analysis identified significant associations between the change in ether lipid species (including alkylphosphatidylcholine, alkenylphosphatidylcholine, lysoalkylphosphatidylcholine, and lysoalkenylphosphatidylcholine) and AD dementia conversion. Specifically, AD dementia converters show a 3–4.8% reduction in these ether lipid species compared to the non-converting CN and MCI groups, suggesting metabolic dysregulation as a key feature of AD progression. Further, The Dementia Risk Model effectively distinguished MCI from AD dementia converters (AUC = 0.70; 95% CI: 0.66–0.74). Within the MCI group, the model identified a high-risk subgroup with a twofold higher likelihood of conversion to AD dementia compared to the low-risk group. External validation in the ASPREE cohort confirmed its predictive utility, with the Dementia Risk Score discriminating incident dementia from cognitively normal individuals (C-index = 0.75, 95% CI: 0.73–0.78), improving prediction by 2% over the combination of traditional risk factors and APOE genetic risk factor.

*Corresponding author. Department of Psychiatry & Behavioral Sciences, Duke University, DUMC Box # 102506, Durham, NC 27710, USA.
E-mail address: lisa.howerton@duke.edu (R. Kaddurah-Daouk).
[o]Equal first author.
[p]Equal senior and corresponding author.
[q]Data used in preparation of this article were obtained from the Alzheimer's Disease Neuroimaging Initiative (ADNI) database (adni.loni.usc.edu). As such, the investigators within the ADNI contributed to the design and implementation of ADNI and/or provided data but did not participate in analysis or writing of this report. A complete listing of ADNI investigators can be found at: http://adni.loni.usc.edu/wp-content/uploads/how_to_apply/ADNI_Acknowledgement_List.pdf.

Additionally, the Dementia Risk Score was significantly associated with reduced temporal lobar fludeoxyglucose uptake ($\beta = -0.286$, $p = 1.34 \times 10^{-4}$), higher amyloid PET levels ($\beta = 0.308$, $p = 4.03 \times 10^{-4}$), and elevated p-tau levels ($\beta = 0.167$, $p = 2.37 \times 10^{-2}$), reinforcing its pathophysiological relevance in tracking neurodegeneration, amyloid burden, and tau pathology.

Interpretation These findings highlight lipidomic profiling as a potential blood-based biomarker for identifying individuals at high risk of AD progression, offering a scalable, non-invasive approach for early detection, risk stratification, and targeted interventions in AD.

Funding The National Health and Medical Research Council of Australia (#1101320 and #1157607); NHMRC Investigator grant (#GNT1197190); Victorian Government's Operational Infrastructure Support Program; National Heart Foundation of Australia, Future Leader Fellowship (#102604), and National Health and Medical Research Council Investigator Grant (#2026325); Investigator grant (#2009965) from the National Health and Medical Research Council of Australia; a National Health and Medical Research Council of Australia Senior Research Fellowship (#1042095); National Institutes of Health grants: P30AG010133, P30AG072976, R01AG019771, R01AG057739, U19AG024904, R01LM013463, R01AG068193, T32AG071444, U01AG068057, U01AG072177, U19AG074879, R01AG069901, R01AG046171, RF1AG051550, RF1AG057452; National Institutes of Health/National Institute on Aging grants RF1AG058942, RF1AG059093, U01AG061359, U19AG063744, and R01AG081322, NIH/NLM R01LM012535; FNIH: DAOU16AMPA.

Keywords: Lipidomics; Alzheimer's disease; Cognitively normal; Mild cognitive impairment; AD biomarkers

Research in context

Evidence before this study

A growing number of studies have defined an close link between the plasma lipidome, measured at a single point in time, and AD dementia and its risk factors. Nevertheless, the temporal dynamics of the lipidomic alterations and their relationship with the progression to AD dementia remains unclear.

A Google scholar search was performed, using the key words "Longitudinal analysis" OR "Alzheimer's disease risk prediction" OR "Dementia risk prediction" OR "AD biomarkers" OR "Metabolomics" AND "Lipidomic". We observed that several studies had developed dementia risk scores using specific lipid classes such as phospholipids or sphingolipids. However, there is a lack of studies that comprehensively evaluate AD risk using a broad lipidomic profile to construct a more holistic and data-driven risk model for dementia risk prediction.

Added value of this study

We performed comprehensive cross-sectional and longitudinal analyses of lipidomic data in the ADNI cohort to delineate the relationships between lipid metabolism and progression to AD dementia. Cross-sectional associations are consistent with previous observations, but we identified two novel strongly associated lipid species driven by anticholinesterase usage. Trajectory analysis revealed differences between AD converters and non-converting CN and MCI, with reduced ether lipid synthesis being a defining characteristic of progression to AD. We further developed a dementia risk classification model to stratify the non-converting MCI group into dementia-like and non-dementia-like MCI based on their lipidomic profiles at baseline. The results demonstrated that the model can efficiently classify MCI into low dementia risk and high dementia risk, with the high AD dementia risk group having two times higher risk of conversion to AD dementia than the low-risk group.

Implications of all the available evidence

These highlight the potential of lipidomic studies to improve our understanding of the relationships between lipid metabolism and progression to AD dementia. Lipidomic profiling also show promise to serve as a blood-based test to identify individuals at higher risk for progressing to AD dementia.

Introduction

Late-onset Alzheimer's disease (AD) is the leading cause of dementia, characterised by the progressive death of neurons and loss of brain structure, usually presenting with memory loss.[1,2] Many risk factors have been identified to collectively modulate risk for AD dementia with advanced age (≥65 years) being the strongest risk factor. Moreover, common genetic risk factors are associated with increased risk,[3] such as the *APOE* ε4 allele and sex, with females being more likely to develop AD (especially at age ≥80 years).[4]

Spanning a period of 15–25 years, individuals progress from CN through MCI to overt dementia.[2] As a transitional state between CN and dementia, MCI has mixed aetiologies with different pathologies, neuropsychological profiles, or biomarker anomalies, often presenting with subtle to mild clinical symptoms.[5,6] The transition from MCI to dementia can take a varying length of time, with some individuals remaining stable or reverting to CN.[2,7] The underlying mechanisms contributing to this heterogeneity remain poorly understood. Biomarker-based MCI stratification has become essential for distinguishing high-risk individuals by integrating fluid biomarkers,[8,9] and neuroimaging.[10] However, these biomarkers are often invasive, time-consuming, and expensive, limiting their widespread clinical application. Additionally, challenges remain in standardising biomarker thresholds and ensuring validation across diverse populations. As a promising alternative, blood-based biomarkers such as the lipidome[11] offer a minimally invasive and potentially scalable approach for MCI risk stratification. However, existing predictive models face challenges such as study design biases, overfitting issues, limited sample size, and a lack of cross-cohort validation. A more accurate and generalisable MCI stratification model, using molecular level information (such as lipidomic profiling), could significantly improve prognostic accuracy at the early stages of disease,[12] which is critical for streamlining clinical trials to shorten drug development cycle and avoiding negative results due to this heterogeneity.

A growing number of studies have defined an intimate link between the plasma lipidome, measured at a single point in time, and AD dementia[13–16] or its risk factors.[17–22] Further, lipidomic alterations in plasma,[23,24] cerebrospinal fluid (CSF),[25] and brain regions such as the cerebral cortex and white matter[26] have been implicated in AD dementia progression, particularly in the transition from MCI to AD. Hyunh et al. (2020)[27] identified 71 plasma lipid species from ether lipids and sphingolipids classes that were significantly associated with future AD risk. Dakterzada et al. (2024)[25] provided evidence that fatty acid dysregulations at both CSF and plasma levels may contribute to the pathogenesis and progression, while Obis et al. (2023)[26] demonstrated that lipidome changes — especially in ether lipids — are more pronounced in white matter than in grey matter at disease progression. Despite these findings, most previous studies have been conducted using cross-sectional datasets, which do not capture longitudinal changes in lipid metabolism. The plasma lipidome is highly dynamic, varying in response to environmental exposures (diet, physical activity)[28–30] and over the longer term with age.[31–34] Similarly, the progression of cognitive impairment may predispose individuals to lifestyle changes (unbalanced diet or physical inactivity).[35,36] These changes will influence peripheral lipid metabolism and may therefore appear to be associated with disease in a cross-sectional analysis (referred to as reverse causation). Longitudinal studies can minimise the impact of reverse causation by defining the relationship between changes in the plasma lipidome prior to AD dementia, during the progression to AD dementia, and following AD dementia diagnosis.

In this study, we performed longitudinal analysis of plasma lipidomic profiles in the Alzheimer's Disease Neuroimaging Initiative (ADNI)-1, -GO and -2 cohorts to delineate the relationships between peripheral lipid metabolism and progression to AD dementia. Using this complex data, we also assessed the utility of plasma lipids to identify MCI individuals at high risk of converting to AD dementia. This assessment was subsequently validated in an external cohort, the Aspirin in Reducing Events in the Elderly (ASPREE) study, to stratify cases of incident dementia from CN individuals.

Methods

Participants

ADNI-1, -2 and -GO (http://adni.loni.usc.edu/) is a longitudinal cohort study, randomly recruiting 1524 individuals over 55 years old at baseline. At intervals of 6–12 months, blood and clinical data were collected from each individual, up to a maximum of 10 years. Lipidomic profiling was performed on all blood samples, with 4873 plasma samples examined from baseline up to the 13th time point (at 10 years followed up). After removing 32 duplicate records, 39 samples that did not match clinical data, 26 samples that did not match clinical lipid measurements, and 46 samples with missing BMI data (Supplementary Figure S1), we retained a total of 4730 samples from 1519 participants. Of these, 1393 participants had plasma lipidome profiling since baseline, while 126 participants only had lipidome profiling at later time points. The detailed repeated measurements of these 1393 participants are summarised in Supplementary Table S1. Most participants had visits at baseline (n = 1393), 12 months (n = 1188) and 24 months (n = 1089), with a decline in participant numbers in other time points (Supplementary Figure S2a). Additionally, most participants had 3 repeated measurements, with fewer individuals having long-term follow-ups beyond seven visits (Supplementary Figure S2b).

The definition of probable AD dementia in ADNI followed the NINDS-ADRDA criteria.[37] In brief, individuals with Mini-Mental State Exam (MMSE) scores between 20 and 26 (inclusive) and a Clinical Dementia Rating Scale (CDR) of 0.5 or 1.0 were classified as AD dementia patients.[38] MCI diagnosis was determined based on a combination of criteria rather than any single measure. Participants were defined as MCI if they met all the conditions including MMSE scores

between 24 and 30, a memory complaint, objective memory loss measured by education-adjusted scores on Wechsler Memory Scale Logical Memory II, a CDR of 0.5, absence of significant levels of impairment in other cognitive domains, and essentially preserved activities of daily living.[39] To distinguish MCI from AD dementia, we required that MCI participants did not exhibit functional impairments that significantly affected their ability to perform daily activities, which is a key feature of AD dementia diagnosis. While an MMSE score of 24 and a CDR of 0.5 could also be observed in early-stage AD, individuals classified as MCI did not meet the threshold for significant impairment across multiple cognitive domains and functional decline, which are necessary for an AD dementia diagnosis. Additionally, we used the ADAS-Cog13 (Total13) cognitive score, a 13-item extension of the original ADAS-Cog, to assess cognitive performance across CN, MCI, and AD dementia. This version includes tasks for delayed recall, executive function, and attention, enhancing sensitivity to cognitive decline.

We further defined the longitudinal status of AD dementia diagnosis group in ADNI. Among the 1393 participants at baseline, we classified the AD diagnosis status into stable diagnosis and AD dementia converters: 1) *Stable diagnosis:* Individuals who were CN at baseline and did not transition into MCI or AD were defined as 'stable CN' (n = 337). Individuals that fell within the MCI classification at baseline but did not proceed into AD dementia within the study time frame were classed as 'stable MCI' (n = 413). Similarly, individuals who remained with an AD dementia diagnosis throughout the study was defined as 'stable AD dementia' (n = 243). *2) MCI converters (ADNI):* In this study, 71 individuals converted from CN to MCI but did not progress further were classified as MCI converters. *3) AD dementia converters:* We defined individuals as AD dementia converters if they were CN or MCI at baseline but progressed to AD dementia at a follow-up time point. A total of 29 CN and 300 MCI enrolled at baseline later converted to AD dementia over the follow-up period. Additionally, 34 participants who entered the study at later time points were cognitively normal at their initial assessment but were later diagnosed with AD dementia. In total, 363 individuals transitioned from either CN or MCI to AD dementia. The distribution of converters across the CN, MCI, and AD groups at all time points is detailed in Supplementary Table S2.

We additionally introduced three AD related biomarkers in ADNI[40]: 1) "AmyPet" (n = 742) – a global cortical amyloid deposition measured from amyloid PET scans as biomarkers of β-amyloid; 2) "pTau" (n = 1009) – CSF phosphorylated tau (p-tau) levels as the biomarker of fibrillary tau; 3) "FDG_Temp" (temporal lobar fludeoxyglucose uptake; n = 1059). In this study, we analysed phosphorylated tau (p-tau) biomarkers in CSF, specifically targeting p-tau181 and p-tau217, which are well-established markers for AD pathology. All the biomarkers are available in the LONI online portal (https://ida.loni.usc.edu/).

The difference in clinical variables, risk factors and AD related biomarkers used throughout this study among diagnostic classifications are summarised in Table 1 for baseline, and Supplementary Table S3 across baseline, 12 months and 24 months.

ASPREE is a large-scale randomised, double-blind, placebo-controlled trial that aimed to evaluate the effects of daily low-dose aspirin on prolonging disability-free survival in 19,114 healthy older adults (aged ≥70 years old).[41–44] As detailed in Supplementary Figure S3, we selected participants from the initial ASPREE cohort who had imputed genotype data after quality control and had no prior diagnosis of dementia. After these criteria were applied, 13,349 participants remained. From this group, we identified a case-cohort subset (n = 3976) by selecting participants with incident dementia (n = 463), coronary artery disease (CAD) (n = 370), or who were homozygote for *APOE* ε4 (n = 168) or *APOE* ε2 (n = 59) with 3033 randomly selected participants. For the analyses in this study, we further refined the sub-cohort to include participants aged 70 years or older of European descent, excluding those genetically related to any other participants. After these criteria were applied, the case-cohort subset (n = 3495) contained incident dementia (n = 402) with an average follow-up of 6.5 years, as well as *APOE* ε4 (n = 149) and *APOE* ε2 (n = 56) homozygotes. The rationale for including CAD and genotype-based enrichment was to align with the broader research question investigating genomic and cardiovascular risk factors in neurodegenerative processes. The differences in clinical variables and risk factors by dementia-related diagnosis group are presented in Table 2.

Several cognitive assessments were administered to participants, including the Modified Mini-Mental State (3MS) test to measure global cognition, the Hopkins Verbal Learning Test-Revised (HVLT-R) for episodic memory, the single letter (F) Controlled Oral Word Association Test (COWAT) for language and executive function, and the Symbol Digit Modalities Test (SDMT) to measure psychomotor speed.[42,45] Incident dementia was defined using a composite set of criteria, rather than relying on a single measure. Participants were classified as having dementia if they met one or more of the following conditions: 3MS score <78 (explaining ≈50% of the dementia diagnosis); a drop of >10.15 points from the predicted score based on their own baseline 3MS adjusted for age and education; a report of memory concerns or other cognitive problems to a specialist; clinician diagnosis of dementia as indicated in the participant's medical records; and prescription of a cholinesterase inhibitor.[42,45]

	Stratified by AD dementia disease status				p values[a]
	Stable CN	Stable MCI	AD dementia converters	Stable AD	
n	337	413	329	243	
Age (years)	74.14 (5.99)	71.85 (7.67)	74.22 (6.85)	74.93 (7.64)	1.32×10^{-08}
Gender (% male)	202 (49.3)	234 (56.7)	195 (59.6)	137 (56.4)	3.04×10^{-02}
HDL-C (mmol/l)	1.54 (0.38)	1.51 (0.37)	1.55 (0.37)	1.54 (0.36)	5.01×10^{-01}
Chol (mmol/l)	4.91 (0.94)	4.98 (0.95)	5.02 (0.96)	5.03 (0.99)	3.70×10^{-01}
Trig (mmol/l)	1.18 (0.56)	1.17 (0.53)	1.17 (0.52)	1.17 (0.48)	9.84×10^{-01}
Fasting (% Yes)	393 (95.4)	398 (96.4)	311 (94.8)	230 (95.0)	7.50×10^{-01}
BMI (kg/m^2)	27.25 (4.85)	27.37 (4.77)	26.59 (4.73)	25.78 (4.12)	9.15×10^{-05}
APOE ε4 (%)[b]					2.81×10^{-36}
0	302 (73.3)	240 (58.1)	120 (36.6)	77 (31.8)	
1	99 (24.0)	140 (33.9)	161 (49.1)	115 (47.5)	
2	11 (2.7)	33 (8.0)	47 (14.3)	50 (20.7)	
Total13[c]	8.30 (3.94)	13.65 (5.75)	19.47 (6.74)	29.09 (7.78)	3.96×10^{-246}
AmyPet[d]	0.79 (0.10)	0.84 (0.12)	0.98 (0.13)	1.01 (0.13)	1.45×10^{-61}
Ptau (log_{10})[e]	2.95 (0.38)	3.05 (0.44)	3.44 (0.46)	3.51 (0.44)	2.40×10^{-52}
FDG_Temp[f]	1.27 (0.11)	1.23 (0.12)	1.15 (0.12)	1.05 (0.14)	3.30×10^{-70}

[a]P values were obtained using either Fisher's exact test for categorical variables or ANOVA for continuous variable. [b]*APOE ε4* = **0**: Individuals with no ε4 allele (non-carriers); *APOE ε4* = **1**: Heterozygous carriers with one ε4 allele; *APOE ε4* = **2**: Homozygous carriers with two ε4 alleles. [c]Total13 is ADAS cog 13 score. [d]AmyPet is a global cortical amyloid deposition measured from amyloid PET scans as biomarkers of β-amyloid. [e]Ptau is CSF phosphorylated tau (p-tau) levels as the biomarker of fibrillary tau. [f]FDG_Temp is temporal lobar FDG uptake.

Table 1: **The basic characteristics of participants in the ADNI study (baseline).**

Lipidomic profiling

The lipid extraction and liquid chromatography–tandem mass spectrometry (LC-MS/MS) methodology, using scheduled multiple reaction monitoring (MRM), was conducted as previously described[20] with the addition of approximately 200 additional lipid species from 17 lipid classes.[33] Serum samples (10 μL) were extracted using a single-phase process comprised of 90 μL of butanol:methanol 1:1 and 10 μL of an internal standard mix containing a mix of non-physiological and stable isotope-labelled lipid standards (Supplementary Table S4).[46] In brief, samples were mixed with the extraction solvent, vortexed and sonicated on a sonicator bath for 1 h. They were subsequently centrifuged, and the supernatant was transferred into glass vials with inserts for mass spectrometry analysis.

Lipidomic profiling in the ADNI study was performed on all plasma samples (n = 4730) using our recently expanded targeted lipidomic profiling strategy comprising of reverse phase liquid chromatography in tandem with a QqQ mass spectrometer (Agilent 6490) operating under dynamic multiple reaction monitoring (dMRM) mode. The solvent comprised of 50% H_2O/30% acetonitrile/20% isopropanol (v/v/v) containing 10 mM ammonium formate and 5 μM medronic acid (Solvent A), and 1% H_2O/9% acetonitrile/90% isopropanol (v/v/v) containing 10 mM ammonium formate (Solvent B).

We utilised a dual column setup, with a stepped linear gradient with a 12.9 min cycle time per sample and a 1 μL sample injection. The solvent analytical gradient was as follows: starting with a flow rate of 0.4 mL/min at 15% B and increasing to 50% B over 2.5 min, then to 57% over 0.1 min, to 70% over 6.4 min, to 93% over 0.1 min, to 96% over 1.9 min and finally to 100% over 0.1 min. The solvent was then held at 100% B for 0.9 min before the solvent was decreased to 15% B over 0.2 min and held until a total of 12.9 min. The next sample was then injected, and the columns alternated. In parallel, the

	Stratified by dementia disease status		p values[a]
	CN	Incident dementia	
n	3093	402	
age (years)	74.84 (4.15)	77.85 (5.03)	$<2 \times 10^{-16}$
Gender (% male)	1469 (47.5)	201 (50.0)	3.72×10^{-01}
HDL-C (mmol/l)	1.58 (0.46)	1.60 (0.48)	4.93×10^{-01}
Chol (mmol/l)	5.25 (0.96)	5.29 (0.97)	3.97×10^{-01}
Trig (mmol/l)	1.33 (0.66)	1.25 (0.61)	2.77×10^{-02}
Family history = Yes (%)	768 (24.8)	128 (31.8)	3.00×10^{-03}
BMI (kg/m^2)	28.05 (4.63)	26.76 (4.20)	1.17×10^{-07}
Aspirin treatment = Yes (%)	1585 (51.2)	210 (52.2)	7.47×10^{-01}
Hyperlipidaemia = Yes (%)	2066 (66.8)	270 (67.2)	9.27×10^{-01}
APOE ε4 (%)[b]			3.69×10^{-11}
0	2268 (73.3)	219 (54.5)	
1	695 (22.5)	164 (40.8)	
2	130 (4.2)	19 (4.7)	

[a]P values were obtained using either Fisher's exact test for categorical variables or ANOVA for continuous variable. [b]*APOE ε4* = **0**: Individuals with no ε4 allele (non-carriers); *APOE ε4* = **1**: Heterozygous carriers with one ε4 allele; *APOE ε4* = **2**: Homozygous carriers with two ε4 alleles.

Table 2: **The basic characteristics of participants in the ASPREE study.**

second column is washed with the following gradient, starting at 15% B, increasing to 100% B over 1 min, held for 4 min before returning to 15% B over 1 min. This was held until a total run time of 12.9 min.

The mass spectrometry conditions were set to as follows: gas temperature, 150 °C, gas flow rate 17 L/min, nebuliser gas 20 psi, sheath gas temperature 200 °C, capillary voltage 3500 V, and sheath gas flow 10 L/min. The conditions for the lipid classes examined are summarised in Supplementary Table S4, and the list of lipid species and classes are in Supplementary Table S5. Overall, there were 781 lipid species from 49 lipid classes reported for the ADNI studies. The ASPREE study (n = 3495) used as the validation study was run under identical chromatographic conditions, but using an Agilent 6495C.

Triacylglycerol species were measured under two sets of transitions, as single ion monitoring (SIM) and neutral loss (NL). SIM measurements provide better relative quantification while NL measurements are more specific and sensitive. In modelling, SIM species were excluded, resulting in 749 lipid species from 48 lipid classes in this study. Of these, 724 species overlapped between ADNI and ASPREE.

Both studies were conducted in batches of 486 samples. Quality control procedures included pooled plasma samples every 20 samples, blanks every 40 samples, and National Institute of Standards and Technology (NIST) Standard Reference Material (SRM) 1950 plasma every 40 samples to monitor instrument performance and data consistency. To correct inter-cohort discrepancies, we applied lipid-specific correction factors, calculated as the ratio between the NIST SRM 1950 reference concentration — defined as the median concentration of 1017 unique NIST SRM 1950 samples aggregated across 24 independent studies — and the median concentration of NIST SRM 1950 samples within each separate cohort.

Additional technical details and instrument parameters are available on our lab website (https://metabolomics.baker.edu.au/method/).

Statistics

In the following analysis, lipid species were log transformed, and standardised to zero mean and unit variance. We introduced the covariate set including age, sex, BMI, *APOE ε4*, high-density lipoprotein cholesterol (HDL-C), total cholesterol (TC), triglycerides (TG), fasting status, study cohort (a categorical variable indicating ADNI-1, ADNI-GO, and ADNI-2), omega-3, and statin status for the following models. In the following analysis, we included these lipoprotein measures (HDL-C, total cholesterol, and triglycerides) as we are seeking to identify lipid species association independent of lipoprotein metabolism. Additionally, to further rule out medication-associated confounders, we identified 423 lipid species significantly associated with statin usage (Supplementary Table S6) and 398 lipid species associated with omega-3 usage (Supplementary Table S7), both after multiple testing correction (linear regressions with corrected $p < 0.05$). Therefore, both medications were included as covariates in our analysis.

ANOVA tests were performed to compare baseline characteristics among different diagnostic groups, as summarised in Table 1 (R package 'tableone' 0.13.2 in R 3.6.2).

Development of a dementia risk model

We sought to use the normalised lipidomic data on stable AD dementia subjects (n = 243) and stable cognitive normal individuals (n = 337) at baseline to build a classification model. The rational for selecting stable CN individuals was to minimise potential confounding from subclinical disease, thereby strengthening the predictive power of the model, which was then tested in an independent cohort. Further, we applied this model to stratify non-converting MCI (n = 413) from AD dementia converters (n = 329). To achieve this, ridge regression models within 5-fold cross-validation framework were created to stratify stable AD dementia from stable CN, optimising C-statistic using the R 3.6.2 package 'glmnet v4.1-4' (Fig. 1). Specifically, we randomly split ADNI data into five folds to create a 5-fold cross-validation framework, iteratively selecting one-fold as the validation set while using the remaining four as the training set. Ridge regression was applied in each iteration to construct two predictive models using different sets of predictors: a) Base model: include age, sex, BMI, *APOE ε4*, HDL-C, total cholesterol, triglycerides, fasting status, cohort (a categorical variable indicating ADNI 1, GO, and 2 phases), omega-3, and statin status; b) Lipidome-based model: incorporate all 747 lipid species in addition to the predictors used in the base model. Since two lipid species, deDE (18:2) and deDE (20:4), were strongly associated with dementia-related medications, these lipids were excluded from the predictor set, resulting in a final model incorporating 747 lipid species (Supplementary Table S8). The improvement in model performance of the dementia risk model over the Base model reflected the added value of the lipidome.

As a validation, we applied the model built on AD and CN groups to the MCI and converters groups in ADNI. Beta coefficients from each cross-validation fold were averaged to create a single model. This model was then applied to the non-converting MCI group to generate the probabilities of the MCI individuals being "dementia-like" or "non dementia-like". In addition, the weights were separately applied to the whole dataset across different time points to generate overall AD dementia risk scores for each individual at each time.

To evaluate the model performance, the Receiver Operating Characteristic–Area Under Curve (AUC) was employed as an evaluation metric to access the

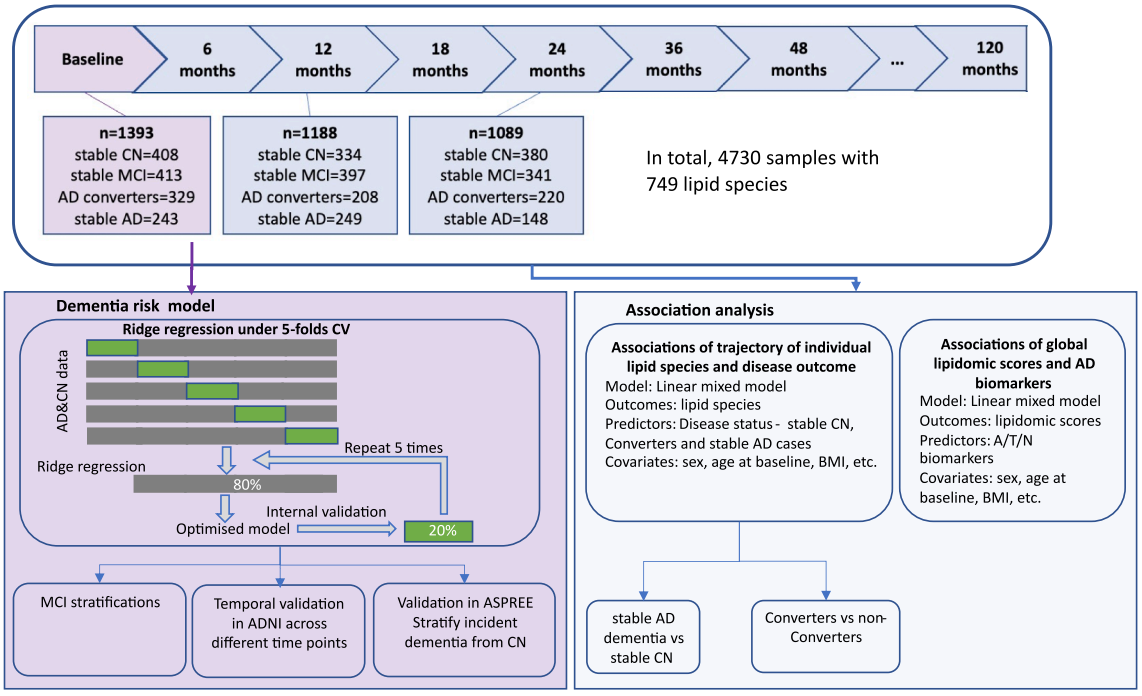

***Fig. 1:* Study design**. This study had two parts. Part 1 involved the development of a Dementia risk model, using baseline data, to characterise the heterogeneity of the non-converting MCI group and to calculate lipidomic risk scores for individuals across different time points. A ridge regression model, built within a five-fold cross-validation framework was used to stratify the non-converting MCI group into dementia-like and non-dementia-like sub-groups. In the development of the model, we treated Dementia risk status as outcome with the predictors including all the lipid species, age, sex, BMI, clinical lipids, fasting status, cohort, *APOE* ε4, omega-3, and statin status. Part 2 was the longitudinal analysis on the repeated measurements across 13 time points to examine the associations of changes in lipid species and lipidomic risk scores with AD dementia status. Associations of the trajectories of individual lipid species and disease outcomes were examined using linear mixed models to undercover the difference of trajectories of lipid species between different groups. The covariates included age, sex, BMI, fasting status, cohort, *APOE* ε4, omega-3, and statin status. Thereafter, global lipidomic scores combing all lipid species derived from the Dementia risk model were fitted into a linear mixed model to define the associations with AD related biomarkers. Similarly, the covariate set included age, sex, BMI, clinical lipids, fasting status, cohort, *APOE* ε4, omega-3, and statin status.

discrimination ability of the models. Additionally, we employed the Net Reclassification Improvement (NRI) metric and Integrated Discrimination Improvement (IDI) to evaluate the reclassification ability of the lipidome-based risk model, compared to traditional risk scores derived from base model. These metrics were calculated using the R 3.6.2 packages 'pROC' 1.18.5 and 'PredictABEL' 1.2–4, respectively. The 95% confident intervals were determined using bootstrapping, with 1000 resamples, ensuring robustness in performance evaluation.

We also performed Kaplan–Meier survival analysis (R 3.6.2 package 'survival' 3.1–12) to evaluate the survival rates (conversion rate to dementia) in high and low dementia risk groups. Differences between groups were evaluated using the log-rank test. In this analysis, the time-to-event was defined as the duration (in months) from baseline to the first recorded AD dementia diagnosis. Individuals who did not develop AD dementia by their last follow-up were right-censored.

External validation of the dementia risk score on a sub-cohort of the ASPREE study

We performed an external validation of the dementia risk score developed in ADNI to access its generalisability and predictive performance. To address potential cohort-specific biases, all lipid data were log10-transformed, and no within-cohort standardisation (e.g., z-scoring) was performed prior to model development. This approach ensured that the lipidomic features retained their absolute scale, thereby avoiding biases introduced by cohort-specific normalisation.

Due to the large mismatch in clinical covariates available between ADNI and ASPREE it was not possible to transfer the lipidome-based model directly into the ASPREE cohort. Thus, for external validation, we first calculated a "Lipidome only risk score" using 722 lipid species shared between ADNI and ASPREE, excluding the two deDE species. This score was derived from all stable AD dementia and CN participants in the

full ADNI baseline dataset and did not include any clinical covariates. The Lipidome only risk score was then calculated in the ASPREE cohort by applying the fixed beta coefficients derived from the ADNI-trained model, without re-training or re-fitting the model in ASPREE.

To assess the predictive performance of the Lipidome only risk score, in ASPREE, relative to traditional risk factors, we compared two cox regression models: a) Base model: including age, sex, BMI, clinical lipids, statin use, aspirin treatment, family history, *APOE ε2*, *APOE ε4*, SBP, DBP, living status, education, diabetes status, smoking, alcohol intake, and depressive symptoms (Center for Epidemiological Studies-Depression-10 [CES-D] scale); and b) Base + Lipidome only risk score: included all variables from the base model, plus the Lipidome only risk score. To assess the model's calibration, we generated calibration plots comparing observed vs predicted dementia probabilities across deciles of risk scores. Calibration was assessed using the time-dependent calibration curves for survival models, using the R 3.6.2 package 'rms' 7.0–0.

Given that the ASPREE study is an incident dementia case-enriched dataset, we employed weighted time-to-event Cox regression model[47] (R 3.6.2 package 'survival' 3.1–12) to assess the incremental predictive value of the lipidome-based model over the base model. Model performance was evaluated using the concordance index (C-index), which, like the AUC, measures discriminative ability but is tailored for right-censored survival data.[48–50] Additionally, hazard ratios (HRs) were used to assess the association between the Dementia Risk Score and incident dementia, after excluding the covariates. Participants were followed from baseline until AD dementia diagnosis, last follow-up, or censoring (due to loss to follow-up or study completion). The time scale for survival analysis was age. To correct for case enrichment, we assigned a weight of 1 to all incident dementia and CAD cases. The remaining cohort samples were weighted based on the ratio of the total eligible population to the number of individuals included in the cohort subset. The proportional hazards (PH) assumption was tested using Schoenfeld residuals to ensure model validity.

We defined the optimal cutoffs for high- and low-risk groups using the Youden Index to maximise discrimination performance. Kaplan–Meier survival analysis (R 3.6.2 package 'survival' 3.1–12) was then conducted to compare survival rates between these groups regarding incident dementia. In this analysis, age was treated as the time scale, and the high- and low-risk groups were used as predictors.

Longitudinal analysis using linear mixed models

We performed longitudinal analyses to examine whether changes in lipid species could predict the AD dementia, where we examined how lipid trajectories differed across AD dementia conversion groups. The analysis aims to characterise metabolic changes associated with AD dementia progression. We applied linear mixed models using repeated measurements across 13 time points to examine the associations between AD dementia diagnosis state and trajectory of lipid species over time. In the model, we treated normalised individual lipid species as the independent variables, and AD dementia diagnosis state as the main predictor and introduced a list of covariates of age (at baseline), sex, BMI, HDL-C, total cholesterol, triglycerides, fasting status, *APOE ε4*, cohort, time point (treated as continuous variable), omega-3, and statin status. The model included an interaction term between time points and AD dementia status, which served as the key term for examining the trajectory of lipid species over time among AD dementia states. The equation of the model is as follows:

$$lipid_i \sim AD * timepoint + age + sex + BMI + HDL + TC + TG + fasting + APOE\varepsilon4 + cohort + omega3 + statin + 1|ID$$

Here, $lipid_i$ is the concentration of each lipid species *i*.

AD presents the AD diagnostic status, such as converters vs non-converters (the combination of stable CN and stable MCI).

timepoint is the continuous variable of time ranging from 1 up to 13.

$AD * timepoint$ include three terms: $AD + timepoint + AD{:}timpoint$. The interaction term of *AD: timepoint* examines the trajectory of lipid species over time points among AD diagnosis status.

age, *sex*, *BMI*, *HDL*, *TC*, *TG*, *fasting* (0/1), *omega3* (0/1), *statin* (0/1), *APOE ε4*, and *cohort* (a categorical variable indicating ADNI 1, GO, and 2 phases) are all treated as covariates in the model.

$1|ID$ is the random effects term, standing for the random intercept for each participant ID.

In the model, we perform two sets of longitudinal analyses on different subsets of the population to: 1) examine the difference in the trajectory of lipid species among AD dementia, CN, and non-converting MCI group (dementia-like or non-dementia-like) using the whole population (excluding the converters); 2) use the changes in lipid species to predict the AD dementia converters on the population excluding all prevalent AD dementia cases. The lme4 package in software R 3.6.2 was used to perform the linear mixed models. Associations were corrected for multiple comparisons using the false discovery rate method of Benjamini Hochberg (BH),[51] using the stats package in software R 3.6.2. Further, verification of linearity assumptions for our linear mixed models was performed using the performance package in software R 3.6.2. Specifically, we

assessed the linearity assumption using scatter plots of residuals vs fitted values, tested Residual normality, and evaluated the Constant variance (homoscedasticity).

Sensitivity analysis

We performed the sensitivity analysis to evaluate whether the trajectories of lipid species within MCI converters behaved similarly as those within AD dementia converters. To do this, linear mixed models were carried out to examine the associations of the trajectory of lipid species with the combination of MCI converters and AD dementia converters relative to non-converting CN and MCI groups.

Ethics

Ethics approval was obtained from the Alfred Hospital Ethics Committee for each cohort. For ADNI, all participants gave written informed consent, and the approval number was (#183/19). For ASPREE, all participants gave written informed consent and the approval number was (#523/21).

Role of funders

The funders had no role in the design and conduct of the study; collection, management, analysis, and interpretation of the data; preparation, review, approval of the manuscript; or decision to submit the manuscript for publication.

Results

As outlined in Fig. 1, we conducted a longitudinal analysis of plasma lipid profiles in the ADNI cohorts to investigate associations between lipidomic changes and progression to AD dementia. Based on these findings, we developed a lipid-based risk model to stratify individuals with MCI by their risk of conversion to AD dementia. The model was externally validated in the ASPREE cohort to assess its ability to predict incident dementia.

Trajectories of lipid species varied between converters and non-converting groups over time

We aimed to examine how individual lipid species longitudinally affect dementia disease progression. To deal with this, we conducted the longitudinal analysis to assess the differences in the trajectories of individual lipid species between AD dementia converters vs non-converters (non-converting CN and MCI) using linear mixed-effects model. The covariate set includes age, sex, BMI, *APOE* ε4, HDL-C, total cholesterol, triglycerides, fasting status, cohort, omega-3, and statin status. The trajectories for 33 lipid species were found to significantly differ between AD dementia converters vs non-converters (Fig. 2a, Supplementary Table S9), based on linear mixed-effects models (FDR-adjusted $p < 0.05$). These lipids were primarily from the LPC(O), LPC(P), and PC(O) classes. To evaluate the impact of clinical lipids and omega3 on the models, we repeated a similar analysis, excluding HDL-C, total cholesterol, triglycerides, and omega-3 from the covariate set. We observed highly consistent findings, with a correlation of β coefficients between the two models of approximately 0.96 (Supplementary Figure S4, Supplementary Table S10). Additionally, we evaluated the key assumptions of the linear mixed models, including linearity, normality of residuals, and homoscedasticity (constant variance of residuals). No major violations of these assumptions were detected. Since 749 sets of linear mixed models were performed for each individual lipid species, reporting all linearity checks is impractical. Instead, we provide representative checks for two key lipid species, LPC(O-18:0) and SM(34:3), as shown in Supplementary Figure S5.

As a sensitivity analysis, we grouped MCI converters with AD dementia converters and compared the trajectories of lipid species against non-converters (Supplementary Figure S6; Supplementary Table S9). Compared to the AD dementia converters only analysis, we observed similar number of lipid species ($n = 34$) showing significantly altered trajectories in the combined AD- and MCI-converter group, based on linear mixed-effects models (FDR-adjusted $p < 0.05$).

When comparing stable AD dementia and CN, only two sphingosine lipid species including Sph (18:1) and Sph (d18:2) showed significantly different trajectories, based on linear mixed-effects models (FDR-adjusted $p < 0.05$) (Fig. 2b; Supplementary Table S11).

Additionally, we carried out linear mixed model analysis for each lipid species to examine within-individual changes over all time points. Of the 749 lipid species analysed, 11 were selected for focused case study. These included lipids with statistically significant longitudinal differences between AD converters and non-converters (FDR-adjusted $p < 0.05$ from linear mixed-effects models; e.g., PE (P-16:0/22:6), PC (O-16:0/16:0)), as well as lipids with known putative biological relevance to AD pathophysiology, such as GM3 (d18:1/24:1), deDE (18:2), AC (12:0), Cer (d18:1/18:0), PI (18:0_22:6), PC (36:4)[+OH], Dimethyl-CE (18:1), dxCA, and CE (24:1). For these selected lipid species, Fig. 3 presents predicted values from models for individuals from AD dementia, CN, and AD converters, demonstrating differential trajectories among diagonal groups. AD dementia and CN showed trajectories in the same direction for most of lipid species (except GM3 (d18:1/24:1)), which is consistent with the results shown in Fig. 2b. Interestingly, the trends of these lipid species in the converter group transitioned from CN concentrations at baseline to AD dementia group concentrations by the end of the study.

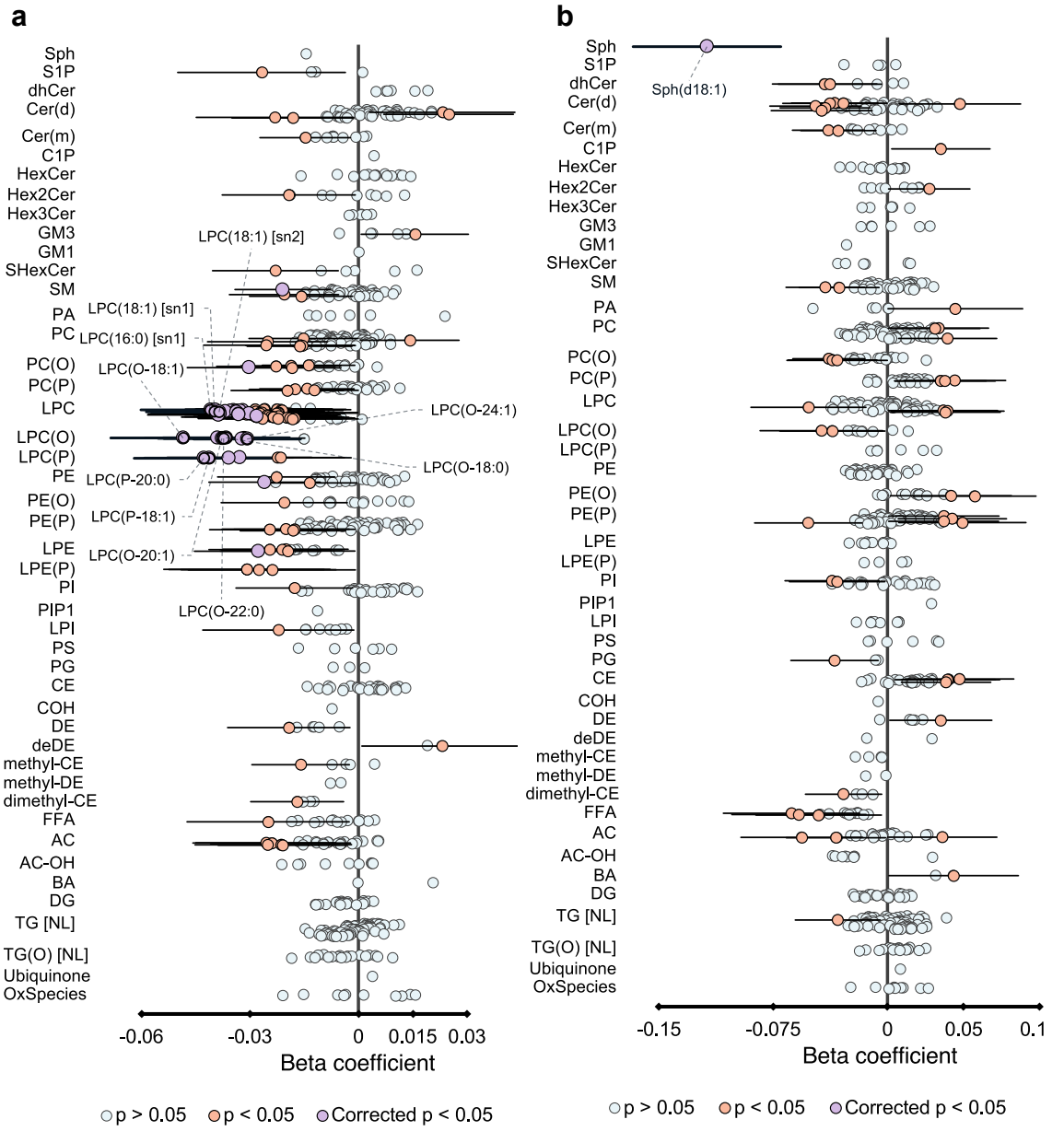

Fig. 2: **Trajectory of lipid species between different AD dementia diagnosis groups across all the time points**. The linear mixed model was performed to examine the association of the changes of individual lipid species with AD dementia diagnosis state. **a)** After excluding AD dementia cases, we compared the converters (n = 363 with 1353 repeated measurements) vs non-converter groups (the combination of non-converting CN and two non-converting MCI groups; n = 776 with 2283 repeated measurements). Beta coefficients represent the interaction between time and conversion status, indicating how lipid trajectories differ between AD converters and non-converters. A positive value suggests a greater increase (or slower decline) in converters; a negative value indicates a steeper decline (or slower increase) relative to non-converters. **b)** After excluding the AD dementia converters, we compared trajectories of lipid species between: AD dementia (n = 261 with 652 repeated measurements) vs non-converting CN (n = 396 with 1049 repeated measurements). Two-sided p-values based on linear mixed model were calculated for each lipid species. In both panels, grey circles indicate non-significant results ($p > 0.05$), orange circles indicate nominal significance ($p < 0.05$ before correction), and purple filled circles indicate significance after Benjamini-Hochberg correction. Each point represents the estimated coefficient with error bars showing the 95% confidence interval. Sphingosine (Sph), Sphingosine-1-phosphate (S1P), Dihydroceramide (dhCer), Ceramide (Cer(d)), Deoxyceramide (Cer(m)), Monohexosylceramide (HexCer), Dihexosylceramide (Hex2Cer), Trihexosylcermide (Hex3Cer), GM3 ganglioside (GM3), Sulfatide (SHexCer), Sphingomyelin (SM), Phosphatidic acid (PA), Phosphatidylcholine (PC), Alkylphosphatidylcholine (PC(O)), Alkenylphosphatidylcholine

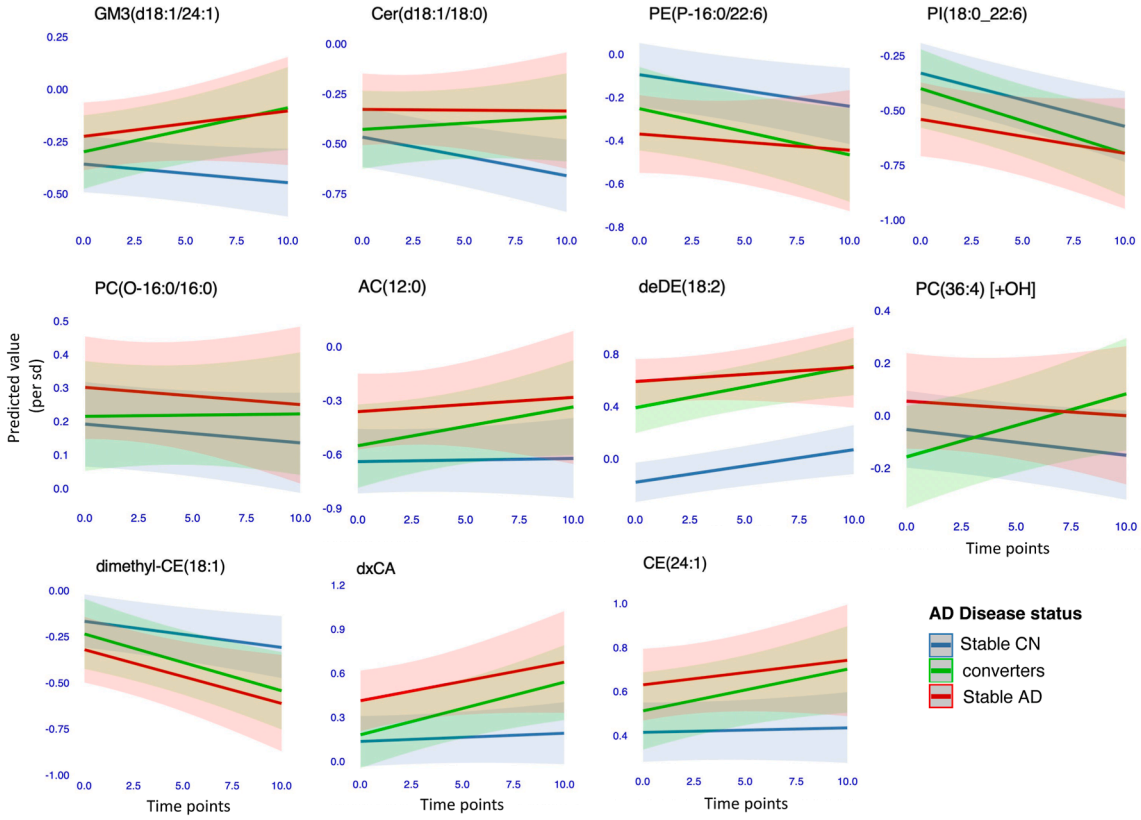

Fig. 3: **The trajectory of selected individual lipid species among different dementia diagnosis groups**. The x-axis denotes time points ranging from baseline (0) to the 10th follow-up visit. The y-axis shows predicted lipid values (in standard deviations of $\log_{10}$-transformed concentrations), estimated using linear mixed models adjusted for baseline age, sex, BMI, fasting status, HDL-C, total cholesterol, triglycerides, cohort, APOE ε4, omega-3, and statin use. Predicted trajectories are shown for three groups: stable AD dementia (n = 261; 652 repeated measurements; red line), converters to AD dementia (n = 363; 1353 repeated measurements; green line), and stable CN individuals (n = 396; 1049 repeated measurements; blue line). The slopes represent the change in lipid levels (standardised $\log_{10}$ concentration) over time within each group. Shaded regions indicate 95% confidence intervals for each trajectory.

Development of a dementia risk model for identification of dementia-like phenotypes in the ADNI cohort

Our previous findings[27] have identified well-defined peripheral signatures associated with prevalent AD dementia, particularly involving lipid pathways such as ether lipids, sphingolipids (notably GM3 gangliosides), phosphatidylethanolamines, and triglycerides. Consistent with these findings, we conducted cross-sectional analyses of lipid species in relation to AD vs CN individuals, accounting for repeated measurements across three time points (baseline, 12 months, and 24 months). Overall, we identified 181 significant associations between lipid species and AD dementia, relative to CN, based on linear regression models (FDR-adjusted $p < 0.05$) (Supplementary Figure S7, Supplementary Table S12). These results further support the role of the lipidome as a strong predictor of dementia risk. Among the most significant associations, two previously unreported lipid species from the dehydrodesmosterol ester (deDE) class—the esterified form of 7-dehydrodesmosterol, a precursor in cholesterol synthesis—exhibited the strongest relationships with AD dementia: deDE (18:2) (beta = 0.77, 95% CI = 0.65–0.88,

(plasmalogen) (PC(P)), Lysophosphatidylcholine (LPC), Lysoalkylphosphatidylcholine (lysoplatelet activating factor) (LPC(O)), Lysoalkenylphosphatidylcholine (plasmalogen) (LPC(P)), Phosphatidylethanolamine (PE), Alkylphosphatidylethanolamine (PE(O)), Alkenylphosphatidylethanolamine (plasmalogen) (PE(P)), Lysophosphatidylethanolamine (LPE), Lysoalkenylphosphatidylethanolamine (plasmalogen) (LPE(P)), Phosphatidylinositol (PI), Lysophosphatidylinositol (LPI), Phosphatidylserine (PS), Phosphatidylglycerol (PG), Cholesteryl ester (CE), Free Cholesterol (COH), Dehydrocholesterol ester (DE), Methyl-cholesteryl ester (methyl-CE), Methyl-dehydrocholesteryl ester (methyl-DE), Dimethyl-cholesteryl ester (dimethyl-CE), Free fatty acid (FFA), Acylcarnitine (AC), Hydroxylated acylcarnitine (AC-OH), Bile acid (BA), Diacylglycerol (DG), Triacylglycerol (TG [NL]), Alkyldiacylglycerol (TG(O)]), Ubiquinone.

$p = 9.76 \times 10^{-32}$, linear regression) and deDE (20:4) (beta = 0.72, 95% CI = 0.59–0.85, $p = 4.19 \times 10^{-23}$, linear regression). However, as outlined in the Methods section, we observed substantial associations between dehydrodesmosterol esters and anti-cholinesterase medication use. Due to potential confounding effects, this lipid class was excluded from subsequent modelling analyses.

Extensive heterogeneity exists within the MCI group, and not all individuals would proceed to develop AD dementia. As we observed substantial lipid associations with prevalent AD dementia, we propose that the plasma lipidome can be leveraged to identify individuals that exhibit an AD dementia like phenotype and would subsequently convert to AD dementia. Using 5-fold cross-validation, we developed a base ridge regression model including demographic and clinical covariates. We then constructed a lipidome-based risk score by adding all lipid species (excluding deDE species) to the base model predictors.

The lipidome-based model effectively distinguished stable AD from cognitively normal (CN) individuals, achieving an AUC of 0.84 (95% CI: 0.81–0.86; Fig. 4a). When applied to the MCI subgroup, where conversion to AD dementia within 10 years was treated as a positive classification, the base model achieved an AUC of 0.65 (95% CI: 0.62–0.68; Supplementary Figure S8), while the lipidome-based model improved discrimination with an AUC of 0.70 (95% CI: 0.66–0.74; Fig. 4b).

To critically evaluate the effectiveness of the lipidome-based risk score in re-stratifying AD dementia converters from MCI individuals, we analysed both categorical and continuous NRI based on the raw counts of the reclassifications, which have direct clinical implications. We evaluated the NRI using different cutoff points ranging from 0.2 to 0.7 (Supplementary Figure S9) and identified that the dementia risk model has the best performance at the cutoff point of 0.6. Relative to the base model, the lipidome-based dementia risk model showed improved reclassification performance. At a cut-off of 0.6, 39% of all AD dementia converters who were initially labelled as low-risk were correctly reclassified to the high-risk group (as shown in Table 3). In contrast, only 0.3% of converters originally classified as high-risk were moved to low-risk. This results in a net reclassification improvement (NRI) of 38.7% for converters, calculated as the proportion of converters moving up minus those moving down. However, for non-converters, the lipidome-based risk model doesn't show improvement over base model: only 1% of all non-converters initially labelled as high-risk were moved down to low-risk, while up to 15% of non-converters initially labelled as low-risk were moved up to high-risk, resulting in a reduced net

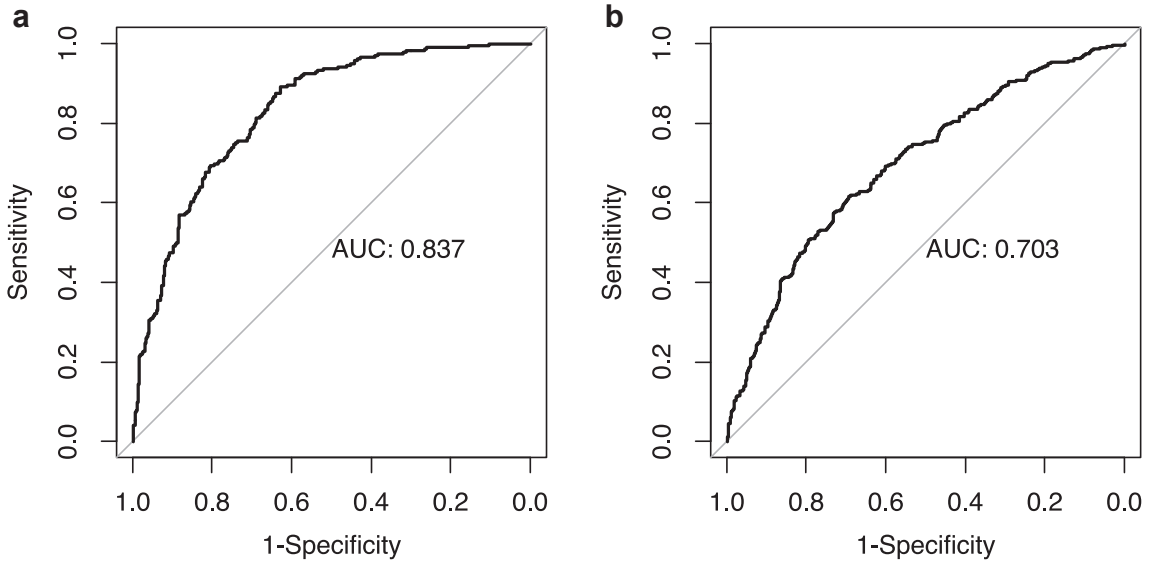

Fig. 4: **Performance of the dementia risk score on the training (the combination of stable AD dementia and CN) (a) and testing set (the combination of stable MCI and AD dementia converters) (b).** Ridge regression model was developed under a 5-fold cross validation framework using stable AD dementia and stable CN groups as the training set and prevalent AD dementia as the outcome. Predictors included the lipidomics measurements, age, sex, BMI, *APOE ε4*, HDL-C, total cholesterol, triglycerides, fasting status, cohort, omega-3, and statin status. **a)** The performance of the model to classify prevalent AD dementia (n = 243) from stable CN (n = 337) in the training set under five-fold cross validation framework was assessed. **b)** The performance of the sample model to classifying risk of AD dementia converters (n = 329) from stable MCI (n = 413) was assessed. The x-axis represents 1–specificity and the y-axis represents sensitivity. Area under the curve (AUC) values were used to quantify model performance.

Raw counts and NRI stats	Events	Non-events
n	329	413
Downward reclassification, n	1	3
Unchanged classification, n	200	347
Upward reclassification, n	128	63
Proportion upward	0.39	0.15
Proportion downward	0.003	0.01
NRI (events or non-events)	0.387	−0.14
	Total NRI	p value
Category NRI	0.24 [0.18–0.31]	$<1.0 \times 10^{-05}$
Continuous NRI	0.51 [0.37–0.65]	$<1.0 \times 10^{-05}$
IDI	0.12 [0.09–0.15]	$<1.0 \times 10^{-05}$

Table 3: **The reclassification performances of lipidome-based AD risk model (relative to base model) to classify incident AD from MCI (NRI and IDI) using the cutoff point of 0.6 in the ADNI cohort.**

reclassification ability of −14% (the proportions of cases moving down minus those moving up).

Overall, the lipidome-based dementia risk score yielded a category NRI of 0.24 (95% CI: 0.18–0.31, $p < 1.0 \times 10^{-05}$, z-test) which included both reclassification of converters and MCI, at the cut-off point of 0.6, and a continuous NRI of 0.51 (95% CI: 0.37–0.65, $p < 1.0 \times 10^{-05}$, z-test). Furthermore, there was an increase in the risk differences between the lipidome-based dementia risk score and base score with an IDI of 0.12 (95% CI: 0.09–0.15, $p < 1.0 \times 10^{-05}$, z-test).

We then estimated the likelihood of being a dementia-like phenotype using the predicted scores from the lipidome-based risk score in each individual. Using a cut-off point of 0.37 (Youden index as illustrated in Supplementary Figure S10), we classified stable MCI and converters into a high or low AD dementia risk category. A greater proportion of participants converted to AD dementia in the high AD dementia risk group relative to the low AD dementia risk group (59%, Fisher's exact test, $p = 1.37 \times 10^{-15}$, Odd Ratio = 3.37, 95% CI = 2.46–4.62; Fig. 5a and b).

Lastly, we investigated classifying the 413 stable MCI individuals into two phenotypic categories. Using the same dementia risk classification cut-off point of 0.37, 276 of the stable MCI individuals were classified into 'non-dementia-like MCI' and 137 individuals were classified into 'dementia-like MCI'.

Comparing dementia-like and non-dementia-like MCI groups, more than 121 lipid species from 26 lipid classes showed signficantly different trajectories, based on linear mixed-effects models (FDR-adjusted $p < 0.05$) (Supplementary Figure S11; Supplementary Table S13). A majority of these were from the SM, GM3, acylcarnitine (AC), alkylphosphatidylcholine (PC (O)), alkenylphosphatidylcholine (PC(P)), LPC, LPC(O), LPC(P), and dehydrocholesterol ester (DE) classes. Of these lipid species, we observed 13 lipid species from the lipid classes of GM3, LPC(O), AC, SM, CE and DE also appeared in the top 50 predictors in the dementia risk model.

Temporal performance of dementia risk model validated across time points in the ADNI cohort

We further applied the dementia risk model built on the baseline AD dementia and CN data to the whole data set across three major time points. We first evaluated the prediction performance of the model to stratify prevalent dementia from CN on each single time point. The predictive performance at the three main time points was AUC: 0.83 (95% CI: 0.80–0.86) at baseline, AUC: 0.898 at 12 months, and AUC: 0.913 at 24 months (Fig. 6a). We further evaluated the ability of the models to stratify converters from MCI across three time points, yielding AUCs of 0.70 (95% CI: 0.66–0.74) at baseline, 0.71 (95% CI: 0.67–0.75) at 12 months, and 0.73 (95% CI: 0.68–0.77) at 24 months (Fig. 6b). The model demonstrated consistent and robust prediction performance at each time point. The distributions of the risk score were described in Supplementary Figure S12.

Dementia risk model can predict incident dementia in a sub-cohort of the ASPREE study

The Dementia Risk Score was externally validated in the ASPREE sub-cohort using a weighted time-to-event Cox regression model to evaluate its predictive performance. Specifically, we assessed the discriminatory ability of the lipidome-based Dementia Risk Score, originally derived from ADNI, to stratify individuals who developed dementia from those who remained cognitively normal in ASPREE. To quantify this, we calculated the C-index, a measure comparable to the area under the curve in survival analysis. We evaluated two cox regression model with different sets of predictors: 1) the Base model including all the conventional risk factors (age, sex, BMI, Statins, aspirin treatment, *APOE* ε4, education, diabetes status, smoking, alcohol intake, and depressive symptoms) and *APOE* genotypes; 2) the Base model + the lipidome only risk score. The C-index of the base model is 0.73 (95% CI = 0.71–0.76). The addition of dementia risk scores to the base model improved the C-index up to 0.75 (95% CI = 0.73–0.78), demonstrating a moderate enhancement in predictive accuracy. Since both cox regression models were built in ASPREE itself, the calibration plot (Supplementary Figure S13) shows strong agreement between predicted and observed dementia risk across all risk score deciles, confirming the reliability of both base model and our dementia risk model.

Additionally, the lipidome only risk score showed a significant association with incident dementia risk with a HR = 1.21 (95% CI = 1.08–1.36) and $p = 9.85 \times 10^{-04}$ (Cox regression) (Fig. 7). Assessment of the proportional hazard assumptions of the Cox model revealed

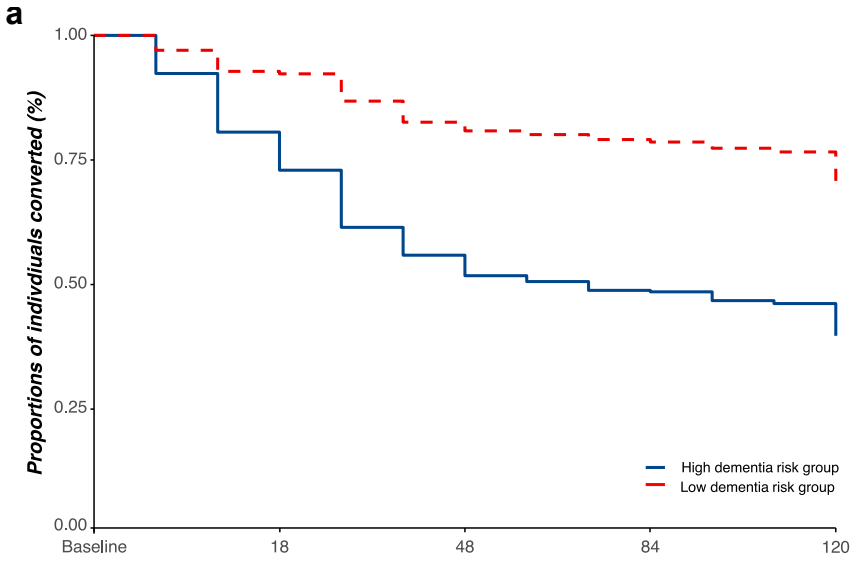

b

	BL	6m	12m	18m	24m	36m	48m	60m	72m	84m	96m	108m	120m
High risk group	343 (0)	343 (27)	316 (40)	276 (26)	250 (40)	210 (21)	189 (14)	175 (4)	171 (6)	165 (1)	164 (6)	158 (2)	156 (19)
Low risk group	399 (0)	399 (11)	388 (17)	371 (2)	369 (21)	348 (15)	333 (7)	326 (3)	323 (4)	319 (2)	317 (2)	312 (3)	309 (33)

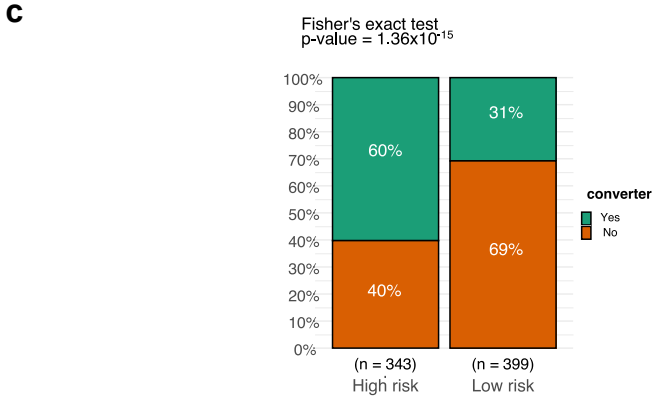

Fig. 5: **The converters non-converting MCI are stratified by the dementia risk score**. **a**) Kaplan–Meier curves were plotted to compare the cumulative incidence of AD dementia conversion over time between individuals in the high-risk (n = 343) and low-risk (n = 399) dementia score groups. Time (in months) is shown on the x-axis, and the cumulative proportion of individuals who converted to AD dementia is shown on the y-axis. This analysis illustrates the temporal dynamics of disease progression and the predictive value of the lipid-based dementia risk score, with divergence between curves indicating stratification performance. **b**) The exact numbers of converters out of the total number of individuals at each time point were detailed in brackets. **c**) Fisher's exact test was used to assess whether the proportion of AD dementia converters differed significantly between the high (n = 343) and low (n = 399) risk groups.

no violations for any of the variables included in the model (Supplementary Table S14).

We stratified the population into high- and low-risk groups, with their respective risk score distributions presented in Supplementary Figure S14a. Further, Kaplan–Meier survival analysis (Supplementary Figure S14b) revealed that individuals in the low-risk group experienced dementia onset approximately 2–3 years later than those in the high-risk group. The survival rate difference between the groups was statistically significant ($p = 3.7 \times 10^{-03}$, log-rank test).

Associations of dementia risk scores with AD related biomarkers in the ADNI cohort

The inclusion of the key AD biomarkers including amyloid deposition measured from AmyPET, CSF p-

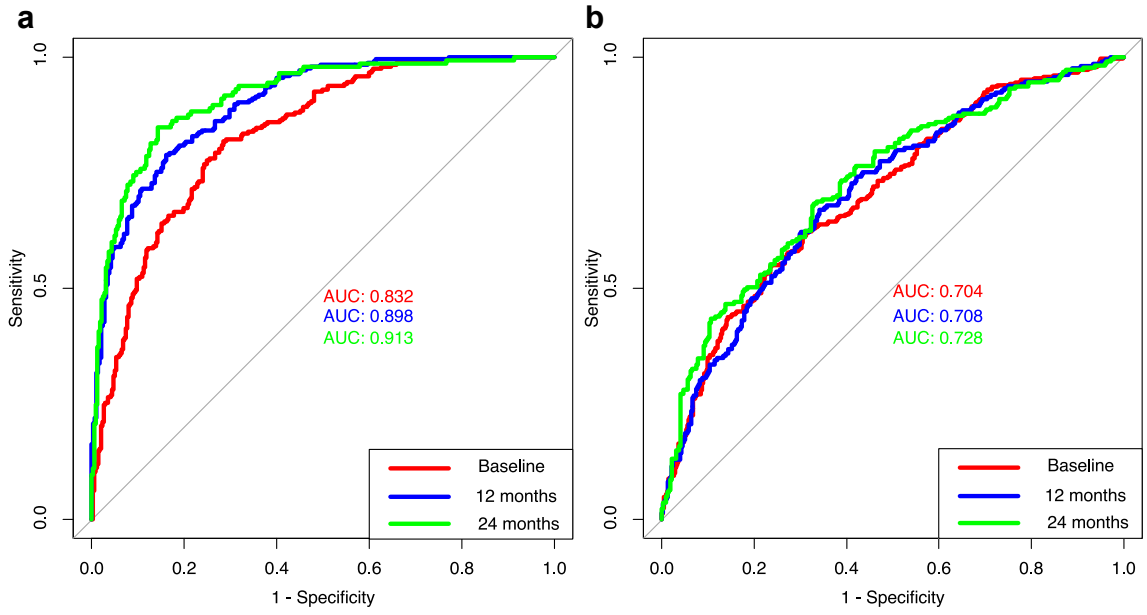

Fig. 6: **The performance of the dementia risk score in AUC across different time points**. **ROC AUC curves** of the risk score to stratify groups **across** baseline (red, n = 1393), 12 months (blue, n = 1188), and 24 months (green, n = 1089). a) Stratifies prevalent AD dementia from CN. b) Stratifies converters from MCI across three time points.

tau, FDG_Temp, and TOTAL13, is essential for understanding how lipidomic alterations reflect established AD pathology or represent independent metabolic risk factors. By integrating these biomarkers, we aim to determine the pathophysiological relevance of the lipidome-based Dementia Risk Score.

To explore these relationships, we conducted a linear mixed-effects model to examine the association between the Dementia Risk Score and AD-related biomarkers, incorporating repeated measurements from baseline, 12 months, and 24 months. The Dementia Risk Score showed significant associations with all AD-related biomarkers. Notably, the strongest association was observed with TOTAL13 cognitive score (beta = 0.489, 95% CI = 0.361–0.617; $p = 8.36 \times 10^{-14}$, linear mixed effects) (Fig. 8). Additionally, the score was negatively associated with FDG_Temp (beta = –0.286, 95% CI = –0.432 to –0.139, $p = 1.34 \times 10^{-04}$, linear mixed effects) and positive associations with AmyPet (beta = 0.308, 95% CI = 0.138–0.478, $p = 4.03 \times 10^{-04}$, linear mixed effects) and p-tau (beta = 0.167, 95% CI = 0.022–0.311, 2.37×10^{-02}, linear mixed effects).

Discussion

We performed comprehensive cross-sectional and longitudinal analyses of lipidomic data in the ADNI cohort to delineate the relationships between lipid metabolism and progression to AD dementia. Cross-sectional associations are consistent with previous observations, though we identified two novel strongly associated lipid species driven by anticholinesterase usage. Trajectory analysis revealed minor differences between subgroups, with reduced ether lipid synthesis being a defining characteristic of progression to AD. Of note, there were many MCI in the ADNI study. While some of these MCI progressed to AD dementia over the follow-up period, others appeared to be stable but displayed heterogeneity in their plasma lipidome, and this was used to stratify these individuals into dementia-like and non-dementia-like MCI. This dementia risk score showed robust performance in predicting risk of AD in ADNI and in external validation. Together, these findings suggest that lipidomic profiling has potential clinical utility as a risk assessment tool.

We investigated the longitudinal changes in the plasma lipidome to gain a deeper understanding of how lipid metabolism evolves in relation to AD development and progression. Lipid trajectories (calculated over 10 years) revealed distinct changes in the plasma lipidome over time. Indeed, multiple lipid species showed different longitudinal trajectories that associated with AD dementia converters relative to the non-converting CN and MCI groups. We identified that 33 lipid species from LPC(O), LPC(P), LPC, and PC(O) classes decreased in concentration in the converter group. There was consistent evidence of decreasing ether lipids for participants in the transition to AD dementia,[23,27] which may reflect changes in the biosynthetic pathway i.e. a gradual deterioration in peroxisome function, leading to decreased ether lipids in circulation.[52] Previous studies have highlighted the role of ether lipids in

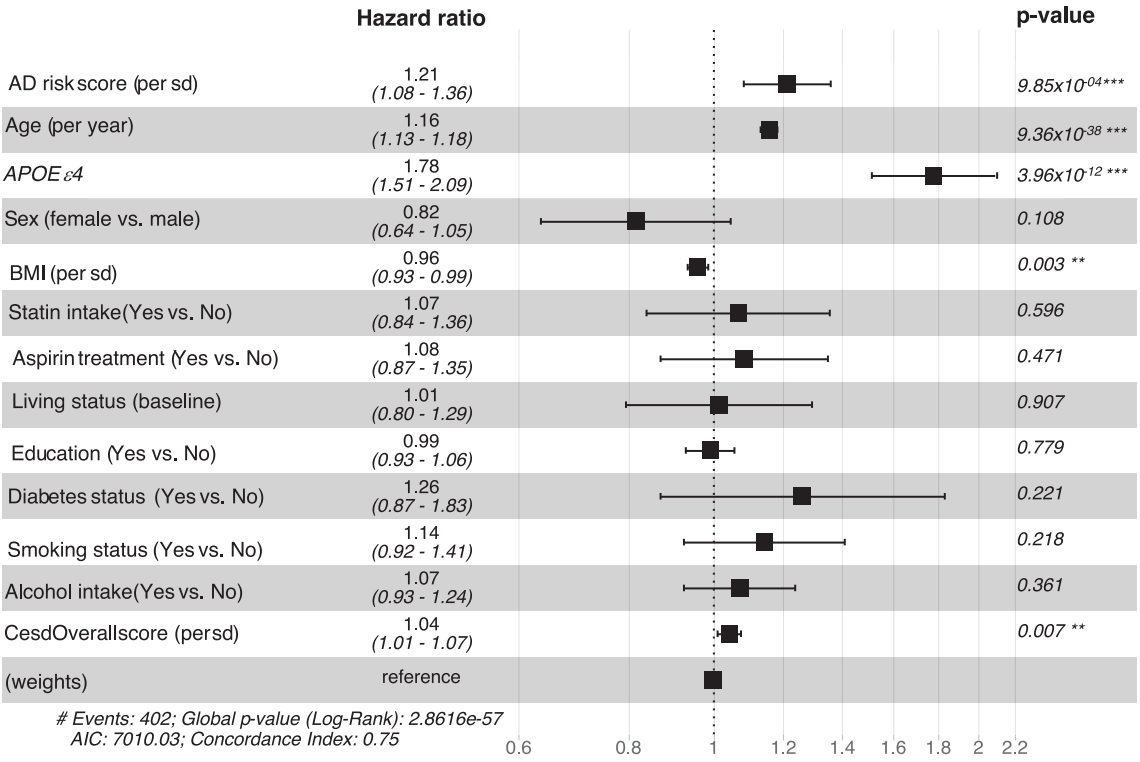

Fig. 7: **The Cox regression model treating incident Dementia as the outcome in the ASPREE cohort**. This figure presents hazard ratios (HRs) from a weighted Cox proportional hazards model assessing the association between the standardised lipidome-based dementia risk score (AD risk score; per 1 SD increase) and incident dementia in the ASPREE cohort (n = 3495). The model was adjusted for age, sex, body mass index (BMI), statin use, aspirin treatment, living status, education, diabetes, smoking, alcohol intake, and depressive symptoms measured by Center for Epidemiological Studies-Depression-10 [CES-D] scale ("CesdOverall score"). Hazard ratios are shown with 95% confidence intervals in brackets. p-Values were derived from Wald tests. Significance is indicated as follows: *p < 0.05, **p < 0.01, ***p < 0.001. The number of events ("#Events:402") is provided. Weights corrected for case-enrichment: dementia/CAD cases were weighted as 1, while non-cases were scaled to reflect their frequency in the full cohort. Model performance was assessed using the concordance index (C-index).

biofluids and brain tissues in the pathophysiological processes of AD dementia and AD progression. Notably, CSF ether-linked TG (O-52:5) was identified as the most influential lipids on the rate of progression from MCI to AD (25). Interestingly, genetic analysis also identified TG (O-52:2) as a mediator for the effects of APOEε2 on AD risk.[22] In addition to biofluids, ether lipid alterations in brain tissues have been linked to dementia progression. A decade ago, researchers identified reduced plasmalogen content in mid-temporal cortex,[53] frontal cortex[54] and white matter[55] as contributors to the AD dementia progressions. In particular, a severe plasmalogen deficiency was observed in white matter across cerebral (temporal, frontal, and parietal) and cerebellar regions at the MCI stage. Consistent with these findings, Obis et al. (2023)[26] reported a downregulation of ether lipids in both grey and white matter, with a more pronounced reduction in white matter as AD progressed.

In our longitudinal analysis, AD dementia converters also showed a downward trajectory in the concentration of lysophospholipids species (containing 16:0, 18:0, 18:1, 20:0, 22:0, 22:1 and 24:0 fatty acids). In support of this observation, several cross-sectional studies have reported that plasma levels of LPC were decreased in the AD dementia patients compared with the healthy group[56] and the LPC-to-PC ratio was also inversely associated with AD dementia,[57,58] suggesting decreasing phospholipase activity as the disease progresses. In humans, LPC(O) and LPC(P) species are metabolised through two distinct mechanisms: they are synthesised as ether lipids via a de novo biosynthetic pathway in peroxisomes, where ether bonds are introduced at the sn-1 position; alternatively, they can arise from the cleavage of plasmalogens by plasmalogen-specific phospholipase A2 (PLA2), which removes the fatty acid from the sn-2 position. Therefore, we hypothesise that both pathways—peroxisome dysfunction[52] and decreased PLA2[59,60]—result in the scarcity of ether-lysophospholipids in participants transitioning to AD dementia. Increased PLA2 activity has been found in many inflammatory diseases,[61] and as

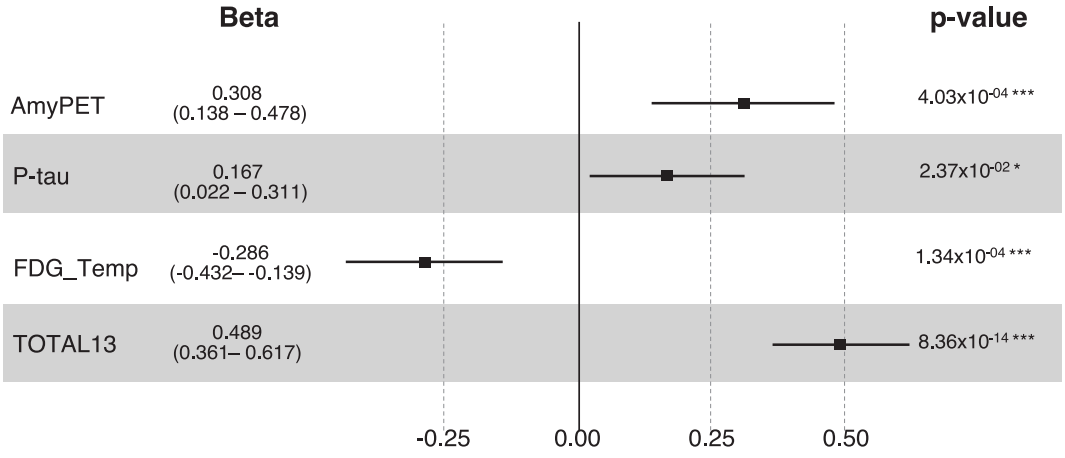

***Fig. 8:* Associations of dementia risk scores with AD dementia related biomarkers**. Linear mixed-effects models were used to assess associations between the standardised lipid-based dementia risk score (per 1 SD increase) and four AD biomarkers: amyloid PET (AmyPET; n = 742), CSF phosphorylated tau (pTau; n = 1009), temporal lobe FDG uptake (FDG_Temp; n = 1059), and ADAS-Cog13 cognitive score (TOTAL13; n = 1310). The x-axis shows standardised effect sizes (βeta), indicating change in each biomarker per 1 SD increase in risk score. Models were adjusted for age (at baseline), sex, BMI, HDL-C, total cholesterol, triglycerides, fasting status, *APOE ε4*, cohort, time point, omega-3, and statin status. p-Values were obtained from fixed effects of the linear mixed models. Significance is indicated as follows: *p < 0.05, **p < 0.01, ***p < 0.001.

neuroinflammation is a hallmark of AD, excessive PLA2 activation may accelerate plasmalogen depletion and impair membrane integrity. Additionally, plasmalogens are particularly susceptible to oxidation which relates to their proposed role as antioxidants, thus loss of plasmalogens may be a response to the elevated oxidative stress in AD.[62] Since peroxisomes regulate lipid metabolism and oxidative balance, their dysfunction may exacerbate oxidative stress and inflammation, further accelerating neurodegeneration.[63] A better understanding of the altered activity of PLA2, peroxisomal dysfunction and ether lipid metabolism could help to identify novel therapeutic targets in AD dementia.[64]

In this study, we developed a dementia risk score using plasma lipidomic profiles which was built using ridge regression within a 5-fold cross validation framework and on the large training dataset (AD dementia and healthy groups; n = 651). The prediction accuracy of the lipidomic model was assessed within the cross-validation framework and gave an AUC of 0.83 for the separation of CN and AD dementia. When applied to participants with MCI (including AD dementia converters), it efficiently classified them into low AD dementia risk and high AD dementia risk, with the high AD dementia risk group having two times higher risk of conversion to AD dementia than the low AD dementia risk group. External validation of the dementia risk model in the APSREE cohort showed that the dementia risk score improves the prediction of incident AD dementia risk. Compared to a traditional but comprehensive dementia risk prediction model (combining conventional risk factors and APOE genotype), the dementia risk score led to a 2% improvement in the C-index. These results suggest that the lipidome-based dementia risk model demonstrates potential for blood-based risk assessment of incident AD dementia, but further validation is needed to confirm its clinical utility, particularly given the moderate improvement in C-index in ASPREE.

Recent advancements in AD biomarker research highlight the potential of fluid-based biomarkers[8,9] including p-tau and neuroimaging,[10] in tracking disease progression. Several advanced studies have also developed dementia risk scores using AD related biomarkers.[65–68] Specifically, Palmqvist et al.[65] and Cullen et al.[66] carried out logistic regression models using a combination of plasma p-tau and other accessible biomarkers to predict incident Alzheimer's disease dementia in BioFinder (n = 340) and ADNI (n = 543; validation cohort). For the subgroup of 106 subject cognitive decline (SCD) and 437 MCI (including 102 Converters) of tADNI, Palmqvist et al.[65] reported an AUC of 0.78 using plasma p-tau181 only and an AUC of 0.91 when combining plasma p-tau181 with traditional risk factors such as APOE, sex, etc. Similarly, Cullen et al.[66] also reported an AUC of around 0.90 to stratify incident AD from others in ADNI, using plasma biomarkers of β-amyloid, tau and neurodegeneration. Another study by Planche et al.[67] validated the performance of blood biomarkers to predict incident dementia risk in the MEMENTO cohort (n = 2323 with subjective cognitive complaint or MCI, and 257 of these converted to dementia during follow-up). This study employed a Cox regression model and identified that blood p-tau181 alone was the best predictor with c-

index = 0.83. The C-index increased to 0.88 when combined with traditional risk factors. Further, a study by Mattsson-Carlgren et al.[68] implemented linear regression to predict rates of longitudinal cognitive change using a range of CSF biomarkers and uptake of Pittsburgh Compound B Positron Emission Tomography, across two cohorts–BioFINDER-1 cohort and WRAP cohort (n = 564 in total). The study demonstrated that p-tau217 was the best marker to predict mPACC slope and MMSE slope. All of these studies demonstrated high performance of these biomarkers in predicting dementia risk. However, due to the limited sample size of the training and validation cohorts, the performance of Cullen et al.,[66] Palmqvist et al.[65] and Mattsson-Carlgren et al.[68] is challenged with heavy overfitting problems. Although Planche et al.[67] has a relatively large sample size, it lacked external validation. In this study, we used a large clinical cohort with 1393 individuals at baseline, and up to 4730 longitudinal plasma samples within 10 year time frame. To avoid overfitting, we carried out five-fold cross validation when reporting performance. We also externally validated our model in a separate large cohort, ASPREE, which included 3495 participants with 402 incident dementia cases. Additionally, while established biomarkers of AD pathology (e.g., tau and amyloid markers) are widely studied, lipidomics presents distinct advantages, including greater accessibility (non-invasive blood-based testing), cost-effectiveness (compared to CSF and PET imaging), and early sensitivity to metabolic changes that may precede amyloid and tau pathology. Additionally, lipid alterations may capture neuroinflammation and membrane integrity loss, offering complementary insights beyond tau biomarkers. Although p-tau 217 remains a leading plasma biomarker, integrating lipidome-based risk scores with tau and neuroimaging markers could enhance predictive accuracy and personalised risk stratification. Future research should explore multi-modal biomarker approaches to optimise AD risk assessment and early intervention strategies.

There are several limitations in this study. Although the study extends up to 10 years, the majority of records are from baseline to 24 months, limiting the statistical power of longitudinal analyses within this shorter follow-up period. Additionally, there is a potential study bias due to the loss of follow-up for some stable CN individuals at later time points. Given that their conversion rate is approximately 9%, it remains uncertain whether some of these individuals would have eventually converted to MCI or AD. To address this limitation, extended follow-up visits are needed for more comprehensive tracking of disease progression. Furthermore, while the lipidomic risk score showed predictive value, its added utility beyond the genetic marker APOE ε4 is modest. Future studies integrating lipid-based risk scores with established AD biomarkers may enhance prediction accuracy and enable more robust risk stratification.

In conclusion, we have performed comprehensive lipidomic analyses using the longitudinal ADNI -1, –2 and -GO cohorts. We developed a novel dementia risk classification model to effectively differentiate high- and low-risk individuals, demonstrating the potential of lipidomics for early risk stratification. The subsequent longitudinal analysis highlighted significant changes in the lipidome over time in individuals who progressed to AD dementia, particularly in ether-lipid metabolism. These highlight the potential of lipidomic studies to improve our understanding of the relationships between lipid metabolism and progression to AD dementia. Lipidomic profiling also shows potential to improve clinical risk assessment and management of older individuals at risk of AD dementia.

Contributors

Meikle, Kaddurah-Daouk and Kastenmüller led the study design team. Wang, Arnold, and Huynh led the statistical analyses presented in this study. Giles, Weinisch and Livera provided statistical suggestions on linear mixed models. Mellett, Duong, Huynh, and Giles supported the acquisition and processing of the lipidomic data for the cohort. Lacaze, McNeil, and Yu were key members of ASPREE team. Arnold, Kastenmüller, Nho, Saykin, Han, Marella, Blach and Kaddurah-Daouk were key members of the ADNI team and represent the Alzheimer's Disease Metabolomics Consortium (ADMC): A complete listing of ADMC investigators can be found at https://sites.duke.edu/adnimetab/who-we-are/. All authors read and approved the final version of the manuscript. All authors had access to the underlying data, which is also available to the scientific community through the ADNI website. ADNI contributed comprehensive longitudinal clinical, cognitive, neuroimaging, and plasma lipidomic data, which were essential for this study.

Data sharing statement

The results presented in this study are based on data from ADNI and ASPREE. ADNI data are publicly available through the AD Knowledge Portal and the Laboratory of Neuro Imaging Image and Data Archive (https://ida.loni.usc.edu/login.jsp). ASPREE data are available from the corresponding authors upon reasonable request.

Declaration of interests

Dr. Kaddurah-Daouk is an inventor on a series of patents on use of metabolomics for the diagnosis and treatment of CNS diseases and holds equity in Metabolon Inc., Chymia LLC and PsyProtix. Prof. Meikle leads the provisional patent "METHODS OF ASSESSING ALZHEIMER'S DISEASE" on the development of dementia risk scores that has been filed with the Serial No. 63/463,808. Gabi Kastenmüller declares equity in Chymia LLC and EMBL-EBI, is the inventor on patents, Philippine Genome Center/Davao Medical School, DAAD/DWIH, and BMBF. Andrew Saykin has received gifts/services from Avid Radiopharmaceuticals, has editorial involvement with Springer-Nature Publishing, and has served on scientific advisory boards for Eisai, Novo Nordisk, and Siemens. Paul Lacaze is supported by a National Heart Foundation of Australia Future Leader Fellowship. Matthias Arnold reports support from NIH/NIA, is a co-inventor on patents, and has equity in Chymia LLC, PsyProtiz, and Atai Life Sciences.

Other authors have declared that no conflict of interest exists.

Acknowledgements

Support was provided by the National Health and Medical Research Council of Australia (#1101320 and 1157607). KH is supported by an NHMRC Investigator grant (GNT1197190). This work was also supported

in part by the Victorian Government's Operational Infrastructure Support Program. AS receives support from multiple NIH grants (P30 AG010133, P30, AG072976, R01 AG019771, R01AG057739, U19 AG024904, R01 LM013463, R01 AG068193, T32AG071444, U01 AG068057, U01 AG072177, and U19 AG074879). BM was supported by the NIH grant R01AG069901, GK was supported by National Institutes of Health/National Institute on Aging grants RF1AG058942, RF1AG059093, U01AG061359, U19AG063744, R01AG069901, U19AG074879 and R01AG081322. KN was supported by NIH/NLM R01LM012535, NIH/NIA U01AG068057, NIH/NIA U01AG072177, NIH/NIA U01AG24904, NIH/NIA U19AG074879. MA is supported by NIH/National Institute on Aging through grants RF1AG058942, RF1AG059093, U01AG061359, U19AG063744, R01AG069901, U19AG074879 and R01AG081322. PL was supported by National Heart Foundation of Australia, Future Leader Fellowship (102604), and National Health and Medical Research Council Investigator Grant (2026325). PJM is supported by Investigator grant (2009965) from the National Health and Medical Research Council of Australia. PJM was also supported by a National Health and Medical Research Council of Australia Senior Research Fellowship (#1042095). Dr. Kaddurah-Daouk receives support from Multiple grants: R01AG046171, RF1AG051550, RF1AG057452, R01AG059093, RF1AG058942, U01AG061359, U19AG063744 and FNIH: #DAOU16AMPA.

The data available in the AD Knowledge Portal would not be possible without the participation of research volunteers and the contribution of data by collaborating researchers.

Data collection and sharing for this project was funded by ADNI (NIH Grant U01 AG024904) and DOD ADNI (Department of Defense award number W81XWH-12-2-0012). ADNI is funded by the National Institute on Aging, the National Institute of Biomedical Imaging and Bioengineering, and through generous contributions from the following: AbbVie, Alzheimer's Association; Alzheimer's Drug Discovery Foundation; Araclon Biotech; BioClinica, Inc.; Biogen; Bristol-Myers Squibb Company; CereSpir, Inc.; Cogstate; Eisai Inc.; Elan Pharmaceuticals, Inc.; Eli Lilly and Company; EuroImmun; F. Hoffmann-La Roche Ltd and its affiliated company Genentech, Inc.; Fujirebio; GE Healthcare; IXICO Ltd.; Janssen Alzheimer Immunotherapy Research & Development, LLC.; Johnson & Johnson Pharmaceutical Research & Development LLC.; Lumosity; Lundbeck; Merck & Co., Inc.; Meso Scale Diagnostics, LLC.; NeuroRx Research; Neurotrack Technologies; Novartis Pharmaceuticals Corporation; Pfizer Inc.; Piramal Imaging; Servier; Takeda Pharmaceutical Company; and Transition Therapeutics. The Canadian Institutes of Health Research is providing funds to support ADNI clinical sites in Canada. Private sector contributions are facilitated by the Foundation for the NIH (www.fnih.org). The grantee organisation is the Northern California Institute for Research and Education, and the study is coordinated by the Alzheimer's Therapeutic Research Institute at the University of Southern California. ADNI data are disseminated by the Laboratory for Neuro Imaging at the University of Southern California.

Metabolomics data is provided by the Alzheimer's Disease Metabolomics Consortium (ADMC) and funded wholly or in part by the following grants and supplements thereto: NIA R01AG046171, RF1AG051550, RF1AG057452, R01AG059093, RF1AG058942, U01AG061359, U19AG063744 and FNIH: #DAOU16AMPA awarded to Dr. Kaddurah-Daouk at Duke University in partnership with a large number of academic institutions. As such, the investigators within the ADMC, not listed specifically in this publication's author list, provided data along with its pre-processing and prepared it for analysis, but did not participate in analysis or writing of this manuscript. A complete listing of ADMC investigators can be found at: https://sites.duke.edu/adnimetab/team/.

Data on lipidome was generated at the Baker Heart and Diabetes Institute, a member of ADMC. Details on the lipid profiling technologies are described at: (https://metabolomics.baker.edu.au/method).

Appendix A. Supplementary data

Supplementary data related to this article can be found at https://doi.org/10.1016/j.ebiom.2025.105826.

References

1 Niccoli T, Partridge L. Ageing as a risk factor for disease. *Curr Biol*. 2012;22(17):R741–R752.
2 Scheltens P, De Strooper B, Kivipelto M, et al. Alzheimer's disease. *Lancet*. 2021;397(10284):1577–1590.
3 van der Lee SJ, Wolters FJ, Ikram MK, et al. The effect of APOE and other common genetic variants on the onset of Alzheimer's disease and dementia: a community-based cohort study. *Lancet Neurol*. 2018;17(5):434–444.
4 Weidner WS, Barbarino P. P4-443: the state of the art of dementia research: new frontiers. *Alzheimers Dement*. 2019;15(7S_Part_28):P1473.
5 Bowler JV. The concept of vascular cognitive impairment. *J Neurol Sci*. 2002;203:11–15.
6 Delano-Wood L, Bondi MW, Sacco J, et al. Heterogeneity in mild cognitive impairment: differences in neuropsychological profile and associated white matter lesion pathology. *J Int Neuropsychol Soc*. 2009;15(6):906–914.
7 Vermunt L, Sikkes SAM, van den Hout A, et al. Duration of preclinical, prodromal, and dementia stages of Alzheimer's disease in relation to age, sex, and APOE genotype. *Alzheimers Dement*. 2019;15(7):888–898.
8 Jack CR Jr, Bennett DA, Blennow K, et al. NIA-AA Research Framework: toward a biological definition of Alzheimer's disease. *Alzheimers Dement*. 2018;14(4):535–562.
9 Karikari TK, Pascoal TA, Ashton NJ, et al. Blood phosphorylated tau 181 as a biomarker for Alzheimer's disease: a diagnostic performance and prediction modelling study using data from four prospective cohorts. *Lancet Neurol*. 2020;19(5):422–433.
10 Ossenkoppele R, Smith R, Mattsson-Carlgren N, et al. Accuracy of tau Positron emission tomography as a prognostic marker in preclinical and prodromal alzheimer disease: a head-to-head comparison against amyloid positron emission tomography and magnetic resonance imaging. *JAMA Neurol*. 2021;78(8):961–971.
11 Proitsi P, Kim M, Whiley L, et al. Association of blood lipids with Alzheimer's disease: a comprehensive lipidomics analysis. *Alzheimers Dement*. 2017;13(2):140–151.
12 Csukly G, Sirály E, Fodor Z, et al. The differentiation of amnestic type MCI from the non-amnestic types by structural MRI. *Front Aging Neurosci*. 2016;8.
13 Chatterjee P, Lim WL, Shui G, et al. Plasma phospholipid and sphingolipid alterations in Presenilin 1 mutation carriers: a pilot study. *J Alzheimers Dis*. 2016;50(3):887–894.
14 Whiley L, Sen A, Heaton J, et al. Evidence of altered phosphatidylcholine metabolism in Alzheimer's disease. *Neurobiol Aging*. 2014;35(2):271–278.
15 Kling MA, Goodenowe DB, Senanayake V, et al. Circulating ethanolamine plasmalogen indices in Alzheimer's disease: relation to diagnosis, cognition, and CSF tau. *Alzheimers Dement*. 2020;16(9):1234–1247.
16 Barupal DK, Baillie R, Fan S, et al. Sets of coregulated serum lipids are associated with Alzheimer's disease pathophysiology. *Alzheimers Dement*. 2019;11:619–627.
17 Smidak R, Kofeler HC, Hoeger H, Lubec G. Comprehensive identification of age-related lipidome changes in rat amygdala during normal aging. *PLoS One*. 2017;12(7):e0180675.
18 Hancock SE, Friedrich MG, Mitchell TW, Truscott RJ, Else PL. Decreases in phospholipids containing adrenic and arachidonic acids occur in the human hippocampus over the adult lifespan. *Lipids*. 2015;50(9):861–872.
19 Weir JM, Wong G, Barlow CK, et al. Plasma lipid profiling in a large population-based cohort. *J Lipid Res*. 2013;54(10):2898–2908.
20 Huynh K, Barlow CK, Jayawardana KS, et al. High-throughput plasma lipidomics: detailed mapping of the associations with cardiometabolic risk factors. *Cell Chem Biol*. 2018;26(1):71–84.e4.
21 Lim WLF, Huynh K, Chatterjee P, et al. Relationships between plasma lipids species, gender, risk factors, and Alzheimer's disease. *J Alzheimers Dis*. 2020;76:303–315.
22 Wang T, Huynh K, Giles C, et al. APOE ε2 resilience for Alzheimer's disease is mediated by plasma lipid species: analysis of three independent cohort studies. *Alzheimers Dement*. 2022;18(11):2151–2166.
23 Dakterzada F, Jové M, Huerto R, et al. Changes in plasma neutral and ether-linked lipids are associated with the pathology and progression of Alzheimer's disease. *Aging Dis*. 2023;14(5):1728–1738.
24 Dakterzada F, Jové M, Cantero JL, Mota-Martorell N, Pamplona R, Piñoll-Ripoll G. The shift in the fatty acid composition of the circulating lipidome in Alzheimer's disease. *Alzheimers Dement*. 2024;20(5):3322–3333.

25 Dakterzada F, Jové M, Huerto R, et al. Cerebrospinal fluid neutral lipids predict progression from mild cognitive impairment to Alzheimer's disease. *Geroscience*. 2024;46(1):683–696.
26 Obis E, Sol J, Andres-Benito P, et al. Lipidomic alterations in the cerebral cortex and white matter in sporadic Alzheimer's disease. *Aging Dis*. 2023;14(5):1887–1916.
27 Huynh K, Lim WLF, Giles C, et al. Concordant peripheral lipidome signatures in two large clinical studies of Alzheimer's disease. *Nat Commun*. 2020;11(1):5698.
28 Hyötyläinen T, Bondia-Pons I, Orešič M. Lipidomics in nutrition and food research. *Mol Nutr Food Res*. 2013;57(8):1306–1318.
29 Morville T, Sahl RE, Moritz T, Helge JW, Clemmensen C. Plasma metabolome profiling of resistance exercise and endurance exercise in humans. *Cell Rep*. 2020;33(13):108554.
30 Iso-Markku P, Kujala UM, Knittle K, Polet J, Vuoksimaa E, Waller K. Physical activity as a protective factor for dementia and Alzheimer's disease: systematic review, meta-analysis and quality assessment of cohort and case–control studies. *Br J Sports Med*. 2022;56(12):701–709.
31 Johnson SC, Koscik RL, Jonaitis EM, et al. The Wisconsin Registry for Alzheimer's Prevention: a review of findings and current directions. *Alzheimers Dement*. 2018;10(1):130–142.
32 Darst BF, Koscik RL, Hogan KJ, Johnson SC, Engelman CD. Longitudinal plasma metabolomics of aging and sex. *Aging*. 2019;11(4):1262–1282.
33 Beyene HB, Olshansky G, Smith Aa T, et al. High-coverage plasma lipidomics reveals novel sex-specific lipidomic fingerprints of age and BMI: evidence from two large population cohort studies. *PLoS Biol*. 2020;18(9):e3000870.
34 Slade E, Irvin MR, Xie K, et al. Age and sex are associated with the plasma lipidome: findings from the GOLDN study. *Lipids Health Dis*. 2021;20(1):30.
35 Ihira H, Sawada N, Inoue M, et al. Association between physical activity and risk of disabling dementia in Japan. *JAMA Netw Open*. 2022;5(3):e224590–e.
36 Floud S, Balkwill A, Reeves GK, Peto R, Beral V. Cognitive and social activities and long-term dementia risk – Authors' reply. *Lancet Public Health*. 2021;6(5):e270.
37 Weiner MW, Veitch DP, Aisen PS, et al. Impact of the Alzheimer's disease neuroimaging initiative, 2004 to 2014. *Alzheimers Dement*. 2015;11(7):865–884.
38 Arnold M, Nho K, Kueider-Paisley A, et al. Sex and APOE ε4 genotype modify the Alzheimer's disease serum metabolome. *Nat Commun*. 2020;11(1):1148.
39 Petersen RC, Aisen PS, Beckett LA, et al. Alzheimer's disease neuroimaging initiative (ADNI). Clinical characterization. *Neurology*. 2010;74(3):201–209.
40 Teunissen CE, Verberk IMW, Thijssen EH, et al. Blood-based biomarkers for Alzheimer's disease: towards clinical implementation. *Lancet Neurol*. 2022;21(1):66–77.
41 McNeil JJ, Nelson MR, Woods RL, et al. Effect of aspirin on all-cause mortality in the healthy elderly. *N Engl J Med*. 2018;379(16):1519–1528.
42 Yu C, Ryan J, Orchard SG, et al. Validation of newly derived polygenic risk scores for dementia in a prospective study of older individuals. *Alzheimers Dement*. 2023;19:5333–5342.
43 McNeil JJ, Woods RL, Nelson MR, et al. Baseline characteristics of participants in the ASPREE (ASPirin in reducing events in the elderly) study. *J Gerontol A Biol Sci Med Sci*. 2017;72(11):1586–1593.
44 Ernst ME, Broder JC, Wolfe R, et al. Health characteristics and aspirin use in participants at the baseline of the ASPirin in reducing events in the elderly - eXTension (ASPREE-XT) observational study. *Contemp Clin Trials*. 2023;130:107231.
45 Riaz M, Huq A, Ryan J, et al. Effect of APOE and a polygenic risk score on incident dementia and cognitive decline in a healthy older population. *Aging Cell*. 2021;20(6):e13384.
46 Alshehry ZH, Barlow CK, Weir JM, Zhou Y, McConville MJ, Meikle PJ. An efficient single phase method for the extraction of plasma lipids. *Metabolites*. 2015;5(2):389–403.
47 Lalanne C, Mesbah M. 5 - survival data analysis. In: Lalanne C, Mesbah M, eds. *Biostatistics and computer-based analysis of Health data using stata*. Elsevier; 2016:101–115.
48 Harrell FE Jr, Califf RM, Pryor DB, Lee KL, Rosati RA. Evaluating the yield of medical tests. *Jama*. 1982;247(18):2543–2546.
49 Uno H, Cai T, Pencina MJ, D'Agostino RB, Wei LJ. On the C-statistics for evaluating overall adequacy of risk prediction procedures with censored survival data. *Stat Med*. 2011;30(10):1105–1117.
50 Yan G, Greene T. Investigating the effects of ties on measures of concordance. *Stat Med*. 2008;27(21):4190–4206.
51 Benjamini Y, Hochberg Y. Controlling the false discovery rate: a practical and powerful approach to multiple testing. *J R Stat Soc Series B Stat Methodol*. 1995;57(1):289–300.
52 Grimm MOW, Kuchenbecker J, Rothhaar TL, et al. Plasmalogen synthesis is regulated via alkyl-dihydroxyacetonephosphate-synthase by amyloid precursor protein processing and is affected in Alzheimer's disease. *J Neurochem*. 2011;116(5):916–925.
53 Ginsberg L, Rafique S, Xuereb JH, Rapoport SI, Gershfeld NL. Disease and anatomic specificity of ethanolamine plasmalogen deficiency in Alzheimer's disease brain. *Brain Res*. 1995;698(1):223–226.
54 Guan Z, Wang Y, Cairns NJ, Lantos PL, Dallner G, Sindelar PJ. Decrease and structural modifications of phosphatidylethanolamine plasmalogen in the brain with alzheimer disease. *J Neuropathol Exp Neurol*. 1999;58(7):740–747.
55 Morris JC. The clinical dementia rating (CDR). *Neurology*. 1993;43(11):2412–a.
56 Lin W, Zhang J, Liu Y, et al. Studies on diagnostic biomarkers and therapeutic mechanism of Alzheimer's disease through metabolomics and hippocampal proteomics. *Eur J Pharm Sci*. 2017;105:119–126.
57 Klavins K, Koal T, Dallmann G, Marksteiner J, Kemmler G, Humpel C. The ratio of phosphatidylcholines to lysophosphatidylcholines in plasma differentiates healthy controls from patients with Alzheimer's disease and mild cognitive impairment. *Alzheimers Dement*. 2015;1(3):295–302.
58 Mulder C, Wahlund LO, Teerlink T, et al. Decreased lysophosphatidylcholine/phosphatidylcholine ratio in cerebrospinal fluid in Alzheimer's disease. *J Neural Transm (Vienna)*. 2003;110(8):949–955.
59 Gattaz WF, Maras A, Cairns NJ, Levy R, Förstl H. Decreased phospholipase A2 activity in Alzheimer brains. *Biol Psychiatry*. 1995;37(1):13–17.
60 Ross BM, Moszczynska A, Erlich J, Kish SJ. Phospholipid-metabolizing enzymes in Alzheimer's disease: increased lysophospholipid acyltransferase activity and decreased phospholipase A2 activity. *J Neurochem*. 1998;70(2):786–793.
61 Cipolla CM, Lodhi IJ. Peroxisomal dysfunction in age-related diseases. *Trends Endocrinol Metab*. 2017;28(4):297–308.
62 Jové M, Mota-Martorell N, Obis È, et al. Ether lipid-mediated antioxidant Defense in Alzheimer's disease. *Antioxidants*. 2023;12(2):293.
63 He A, Dean JM, Lodhi IJ. Peroxisomes as cellular adaptors to metabolic and environmental stress. *Trends Cell Biol*. 2021;31(8):656–670.
64 Llano DA, Devanarayan V. Serum phosphatidylethanolamine and lysophosphatidylethanolamine levels differentiate Alzheimer's disease from controls and predict progression from mild cognitive impairment. *J Alzheimers Dis*. 2021;80(1):311–319.
65 Palmqvist S, Tideman P, Cullen N, et al. Prediction of future Alzheimer's disease dementia using plasma phospho-tau combined with other accessible measures. *Nat Med*. 2021;27(6):1034–1042.
66 Cullen NC, Leuzy A, Palmqvist S, et al. Individualized prognosis of cognitive decline and dementia in mild cognitive impairment based on plasma biomarker combinations. *Nat Aging*. 2021;1(1):114–123.
67 Planche V, Bouteloup V, Pellegrin I, et al. Validity and performance of blood biomarkers for Alzheimer disease to predict dementia risk in a large clinic-based cohort. *Neurology*. 2023;100(5):e473–e484.
68 Mattsson-Carlgren N, Salvadó G, Ashton NJ, et al. Prediction of longitudinal cognitive decline in preclinical Alzheimer disease using plasma biomarkers. *JAMA Neurol*. 2023;80(4):360–369.